NANOANT4FOOD- Antocianinas Nanoestruturadas – soluções naturais e sustentáveis para melhorar a Qualidade Alimentar e a Saúde

Tomás de Azevedo Garrido
Master's degree in Food Science and Technology
Chemistry and Biochemistry Department
2022

Supervisor
Doctor Ana Fernandes, LAQV – REQUIMTE, Faculty of Sciences of the University of Porto
Co-supervisor
Professor Doctor Victor de Freitas, Faculty of Sciences of the University of Porto

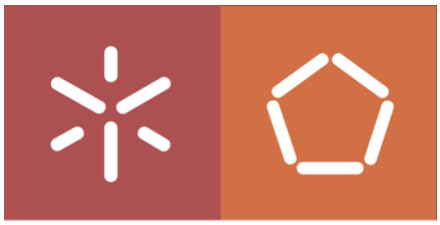

Universidade do Minho
Escola de Engenharia

U.PORTO
FACULDADE DE CIÊNCIAS
UNIVERSIDADE DO PORTO

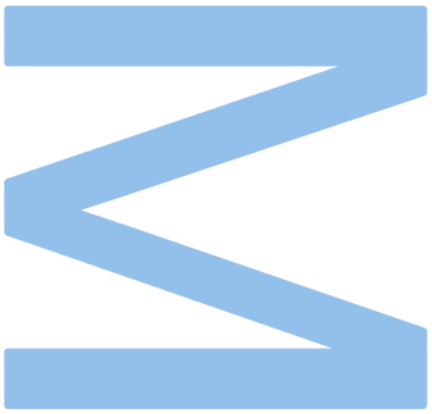

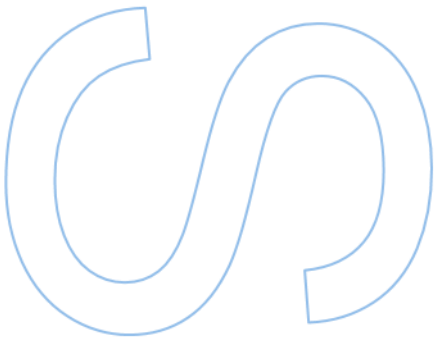

Declaração de Honra

Eu, Tomás de Azevedo Garrido, inscrito no Mestrado em Tecnologia e Ciência Alimentar da Faculdade de Ciências da Universidade do Porto declaro, nos termos do disposto na alínea a) do artigo 14.º do Código Ético de Conduta Académica da U.Porto, que o conteúdo da presente dissertação reflete as perspetivas, o trabalho de investigação e as minhas interpretações no momento da sua entrega.

Ao entregar esta dissertação declaro, ainda, que a mesma é resultado do meu próprio trabalho de investigação e contém contributos que não foram utilizados previamente noutros trabalhos apresentados a esta ou outra instituição.

Mais declaro que todas as referências a outros autores respeitam escrupulosamente as regras da atribuição, encontrando-se devidamente citadas no corpo do texto e identificadas na secção de referências bibliográficas. Não são divulgados na presente dissertação quaisquer conteúdos cuja reprodução esteja vedada por direitos de autor.

Tenho consciência de que a prática de plágio e auto-plágio constitui um ilícito académico.

Tomás de Azevedo Garrido

Porto, 29 de Setembro de 2022

Acknowledgments

This work would not be possible without the help and support of several people, who were directly connected to my work. I would like to thank:

Professor Doctor Victor de Freitas, my supervisor, for all the help and understanding shown during the work done. Doctor Ana Fernandes, my supervisor, for all her contribution during this project. Thank you for making me grow as a person and as a scientist; for making me see that we can always learn in any situation in the laboratory; for your patience to help me in any doubt and to give your opinion to any idea related to the project. To Rodolfo, Francisco, Mónica, Leonor, Sofia, Alexandra, and Catarina, who were always available to listen to me when things were not going so well, but also for making me smile and laugh at any moment of the day. To the members of the Food Polyphenol Lab, for the help and availability they always showed when I needed it.

I would like to thank my family, especially my parents and grandparents, for always doing the possible and impossible to make things go well in my academic path. Without you, clearly none of this would be possible. I know you will be very happy and proud that I was able to get a master's degree after all the difficulties and storms you went through so that I could get the opportunity to study.

I would also like to thank some people who, despite not being directly connected to my work, certainly had a positive impact on the realization of this work and helped me along my academic path.

To Tiago, for having the patience to listen to my problems, my stupid ideas and for giving me the heads up when things were going wrong. Since the first year of my degree with me, I know I will always have a shoulder to lean on when I need it. To Mafalda, Bia, Carolina, Rita, Catarina, Moura, Júlio, Diogo, for making this whole journey easier, whether it be with emotional support, or all the fun moments we spent together. I know I can count on you for everything I need. To everyone that belong to the academic musical group of the Faculty of Science of the University of Porto, thank you for your support, friendship, brotherhood during these five years. To Márcia, for being the most special person that I had the opportunity to meet and that made my journey seem easier. Thank you all for all the patience that you had in the last 4 years. **Thank you all for your support!**

“Right place, right time, right track.”

Resumo

As antocianinas são pigmentos hidrossolúveis que pertencem à classe dos compostos polifenólicos, e são responsáveis pela cor vermelha, azul e roxa de frutos, vegetais e flores. Para além das características cromáticas, as antocianinas possuem propriedades benéficas para a saúde, nomeadamente atividade antioxidante, anti carcinogénica, antidiabética e efeitos na prevenção da obesidade. No entanto, quando estes pigmentos naturais se encontram na forma livre, após extração das matrizes vegetais, a sua estabilidade físico-química é reduzida. A formação de complexos polieletrónicos (PECs) com biopolímeros, poderá ser uma abordagem para a estabilização destes pigmentos. O principal objetivo deste trabalho consistiu na estabilização de um extrato antociânico obtido a partir de amoras, através da formação de PECs insolúveis com um polissacárido sulfatado, o λ-carragenano. Além disso, foi realizada uma caracterização físico-química dos complexos insolúveis preparados.

A caracterização físico-química do extrato de amora revelou que 65 mg. g^{-1} de extrato era de proteína, 557 mg. g^{-1} de extrato correspondeu a antocianinas e 73 mg. g^{-1} foi de compostos fenólicos de baixo peso molecular. A antocianina maioritária detetada foi a cianidina-3-*O*-glucósida. As condições ótimas de formação de PECs insolúveis determinadas baseou-se no uso de um rácio de massa de 1/0.05 (extrato de amora/λ-carragenano), em tampão acetato 10 mM a pH=3. Nestas condições, 12.26 ± 1.68% das antocianinas no extrato participaram na formação de PECs insolúveis. Pela análise de morfologia destes complexos, foi possível verificar que estes apresentam uma superfície compacta e porosa, tendo também sido verificada uma morfologia semelhante a hidrogéis antes da sua liofilização. A complexação foi confirmada por FTIR-ATR, onde se verificou desvios de número de onda e de intensidade, no espectro dos PECs insolúveis, nas bandas referentes aos grupos sulfitos do λ-carragenano, e do grupo C=O do anel benzopirânico. O estudo de estabilidade térmica demonstrou que a complexação aumentou a estabilidade dos pigmentos do extrato de amora. Por fim, a libertação de antocianinas dos PECs, revelou que usando PBS e água a pH=1.7, ocorreu uma libertação drástica até a primeira hora de ensaio, onde a partir desse momento, a libertação por hora é cada vez menor. Água a pH=7.4 revelou uma tendência crescente a partir da primeira hora, enquanto MES e água a pH=5.4 tiveram uma libertação constante a partir da meia hora. Os dados referentes à libertação de ANCs foram aplicados no modelo de Korsmeyer-Peppas, de modo a descrever o tipo de libertação que ocorre nos diferentes meios. Na libertação ocorrida em água a pH=5.4, 7.4 e MES, foi verificado que as ANCs se libertavam seguindo a difusão de Fick, uma

vez que o coeficiente de difusão (n) registado foi abaixo de 0.43. A pH=7.4, houve influência da composição salina e força iónica na libertação de ANCs, uma vez que a mudança para um meio com maior força iónica (PBS), resultou numa mudança no comportamento de libertação. A pH=5.4, é possível constatar que não houve influência da adição de um meio diferente (MES), uma vez que as taxas de libertação são semelhantes. Neste trabalho foram produzidos complexos insolúveis de ANCs-λ-carragenano que poderão ser aplicados na indústria alimentar como corantes insolúveis, produção de biofilmes para formação de novas embalagens, ou de um mecanismo de melhoria da bio acessibilidade de ANCs.

Palavras-chave: Antocianinas, complexos polieletrónicos, morfologia, estabilidade térmica, taxa de libertação, estabilização química, bioatividade.

Abstract

Anthocyanins are water-soluble pigments belonging to the class of polyphenolic compounds responsible for the red, blue, and purple colour of fruits, vegetables, and flowers. In addition to their chromatic characteristics, anthocyanins have beneficial properties to health, namely antioxidant activity, anti-carcinogenic, anti-diabetic, and obesity prevention effects. However, when these natural pigments are found in free form, after extraction from vegetable matrices, their physicochemical stability is reduced. The formation of polyelectronic complexes (PECs) with biopolymers may be an approach to stabilize these pigments. The main objective of this work was the stabilisation of an anthocyanic extract obtained from blackberries, through the formation of insoluble PECs with a sulphate polysaccharide, λ-carrageenan. Furthermore, a physicochemical characterization of the prepared insoluble complexes was performed.

The physicochemical characterization of the blackberry extract revealed that 65 mg. g^{-1} of extract was protein, 557 mg. g^{-1} corresponded to anthocyanins and 73 mg. g^{-1} was attributed to low molecular weight phenolic compounds. The major anthocyanin detected was cyanidin-3-*O*-glucoside. The optimal conditions for the formation of insoluble PECs determined were based on the use of a mass ratio of 1:0.05 (blackberry extract: λ-carrageenan), in 10 mM acetate buffer at pH=3. Under these conditions, 12.26 ± 1.68% of the anthocyanins in the extract resulted in the formation of insoluble PECs. By the morphology analysis of these complexes, it was possible to verify that they present a compact and porous surface, while also having a morphology like hydrogels before freeze-drying. The complexation was confirmed by FTIR-ATR, where it was verified deviations of the wavenumber and intensity, in the spectrum of the insoluble PECs, in the bands referring to the sulphite groups of the λ-carrageenan, and the C=O group of the benzopyran ring. The thermal stability study showed that the complexation increased the stability of the blackberry extract pigments. Finally, the release of anthocyanins from the PECs, revealed that using PBS and water at pH=1.7, a release occurs until the first hour of assay, where from that moment, the release per hour decreases. Water at pH=7.4 revealed an increasing trend from the first hour, while MES and water at pH=5.4 had a constant release from the half hour. The data concerning the release of ANCs were applied to the Korsmeyer-Peppas model to describe the type of release occurring in the different media. In the release occurring in water at pH=5.4, 7.4 and MES, it was found that ANCs were released following Fick diffusion, since the coefficient of diffusion was lower than 0.43. At pH=7.4, there was an influence of the salt composition and ionic strength on the release of ANCs, since switching to a medium with higher ionic strength

(PBS), there was a change in the release behaviour. At pH=5.4, there was no influence of adding a different medium (MES), as the release rates are similar. In this work, insoluble complexes of ANCs-λ-carrageenan were produced, that could be applied in the food industry as insoluble dyes, production of biofilms for formation of new packaging, or a mechanism to improve the bioaccessibility of ANCs.

Keywords: Anthocyanins, polyelectronic complexes, morphology, thermal stability, release rate, chemical stabilization, bioactivity.

Table of contents

Figure Index

Table Index

List of abbreviations

ANC	Anthocyanins
BbE	Blackberry extract
BbE - λ-CRG	Anthocyanins from blackberry extract - λ-carrageenan complexes
BbE/λ-CRG	Weight ratio of anthocyanins from blackberry extract and λ-carrageenan
CRG	Carrageenan
Cy3glc	Cyanidin-3-*O*-glucoside
DPPH	2,2-diphenyl-1-picrylhydrazyl
DSC	Differential Scanning Calorimetry
DTG	Derivate thermogravimetry
ELS	Electrophoresis Light Scattering
FRAP	Ferric Reducing Antioxidant Power
FTIR-ATR	Fourier Transform Infrared Spectroscopy by Attenuated Total Reflection
HPLC	High Performance Liquid Chromatography
HPLC-DAD	High Performance Liquid Chromatography with diode array detector
ι-CRG	ι-carrageenan
λ-CRG	λ-carrageenan
O.D	Optical dispersion
PECs	Polyelectrolyte complexes
STA	Simultaneous Thermal Analysis
TGA	Thermogravimetry analysis
T_{peak}	Temperature where maximum degradation occurs
T_{onset}	Minimum temperature of degradation
Trolox	6-Hydroxy-2,5,7,8-tetramethylchromane-2-carboxylic acid
UV-Vis	Ultraviolet visible
ζ-potential	Zeta potential

Introduction

Framework

The consumption of fruits and vegetables has a crucial function in human life and wellbeing. The main reason is that these natural products have a significant amount of phytochemicals, such as phenolic compounds, that have a positive impact in the human metabolism. On the other hand, in most cases, only the flesh of fruits and vegetables is consumed, resulting in a high quantity of food waste in the form of seeds and peels with a relevant concentration on dietary fibers, polyphenols, and other important nutrients (Sagar et al., 2018). Reusing this type of food wastes can be a reliable way to obtain phytochemicals that can be incorporate into food products and add nutritional value to them (Dordevic et al., 2015; Sagar et al., 2018).

The concept of implementing a greener economy along all the chains of food production can be accomplished by reusing food waste. Nowadays, this attracts consumers to pursue sustainable foods, resulting in a higher innovation in the food industry for food waste that can be incorporated as natural additives or nutraceuticals (Albuquerque et al., 2021). Besides that, food products can be perceived as not only giving nutritional value but also maintaining a better lifestyle, being particularly useful in reducing the impact of highly industrialized food production on the environment (Carocho et al., 2015).

Color is the first quality parameter perceived in food products, affecting consumers' choices. Hence, additives such as colorants are highly used for final product valorization. In the food industry, food colorants are commonly used in the synthetic form since it presents a lower cost of manufacturing and higher stability (Albuquerque et al., 2021). However, synthetic molecules have been associated with toxicity, allergic reactions, behavioral and neurocognitive effects. Natural-based colorants such as betalains, anthocyanins, and carotenoids, obtained from natural sources, can be viewed as new alternatives. Along with the colorant power that these compounds present, they also display several health benefits (Korkina & Kostyuk, 2012). Anthocyanins, naturally present in vascular plants, are water-soluble pigments, that belong to the flavonoids group of polyphenols, and provide them a high range of intense colors (Castañeda-Ovando et al., 2009). Due to their coloring capacity and low toxicity, these molecules can be seen as natural alternative to the synthetic pigments (Alexandra Pazmiño-Durán et al., 2001). Besides that, anthocyanins have been reported to present potential health effects such as prevention of cardiovascular diseases, reduction of diabetes, or antimicrobial activity (Khoo et al., 2017). On the other hand, the low bioavailability, difficulty of extraction, and challenging incorporation into food, can be a

hindrance to the use of these phytochemicals as a novel food ingredient (Castañeda-Ovando et al., 2009). In this sense, developing new methodologies and approaches to increase anthocyanins stability, so that their coloring potential can be used to enhance the organoleptic properties of foods, and to retain their biological activity, is of upmost importance for the food industry.

1. Polyphenols

Polyphenols are plant secondary metabolites, present in various vegetable sources. Several fruits, such as apples, berries ,and cherries can have in their constitution around 200 mg of polyphenols per 100 g of fresh weight (Pandey & Rizvi, 2009). Besides that, some vegetable-based food and beverages, such as chocolate, cereals, red wine, tea, and fruit juices can also be a great source of polyphenols (Pandey & Rizvi, 2009). Polyphenols can have important functions in food products, contributing to color, odor, flavor, and bitterness and in some cases, in red wine, can impart its characteristic astringency (Soares et al., 2012). Polyphenols present themselves with relevant physiological activity, being involved in the protection of plants against ultraviolet radiation and with antimicrobial activity (Pandey & Rizvi, 2009). Besides that, the vibrant color and odor that originate from these molecules, attracts pollinators, therefore, having a direct impact on the proliferation of spores and seeds (Panche et al., 2016).

Regarding their chemical structure, polyphenols are structures that have one or more aromatic rings with at least one substituted hydroxyl group, with their derivatives also having different substituents. This structural diversity arises to two distinct groups of polyphenols, the flavonoids and the non-flavonoids, the former being the most abundant group in nature.

1.1. Non-flavonoids

Non-flavonoids present a simpler chemical structure, with a single aromatic ring with at least a hydroxy group and one or more carbons connected to the aromatic ring (Durazzo et al., 2019). The most abundant classes of non-flavonoids are phenolic acids, including the benzoic acids and cinnamic acids (Amarowicz et al., 2009). Other types of non-flavonoid's include the xanthones, lignans, and stilbenes. These types of molecules have at least two aromatic rings in their chemical backbone (Durazzo et al., 2019). Generally, fruits and vegetables have free phenolic acids in their composition, while cereals and grains have different derivates originating from polymerized phenolic acids (Chandrasekara & Shahidi, 2010). Non-flavonoids have a wide distribution in nature and can be associated with different health benefits, as detailed in Table 1.

Table 1- Non flavonoids' general structure and food sources found in the literature.

Chemical structure	Food sources and potential applications	Reference
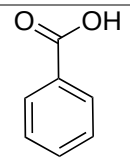 Benzoic acid	Green coffee beans contain a benzoic acid derivate, chlorogenic acid, that can have effects as an anti-inflammatory agent and anti-diabetic.	(Tajik et al., 2017)
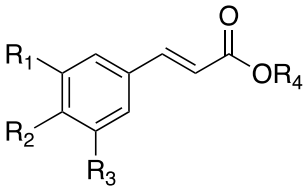 Cinnamic acid	Cinnamon oil showed potential antibacterial effects in gram-negative bacteria.	(Vasconcelos et al., 2018)
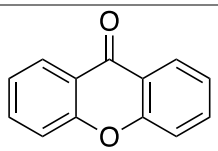 Xanthone	α-Mangostin derived from mangosteen showed antibacterial, anti-inflammatory, and anti-malarial activity.	(Chen et al., 2018)
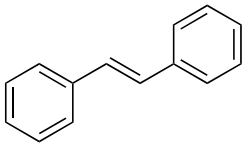 Stilbene	Resveratrol, a stilbene present in peanuts or pistachios, showed anti-inflammatory and anti-cancer activity.	(Tsai et al., 2017)
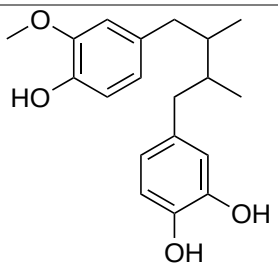 Lignans	The consumption of lignans-rich foods, such as sesame and flax seeds, can contribute to the reduction of breast cancer or colon cancer	(Rodriguez-Garcia et al., 2019)

1.2. Flavonoids

Flavonoids are the most abundant group of polyphenols, being highly diversified in terms of its chemical structure and presence in vegetal sources. For instance, coffee, tea, chocolate, fruits are a great source of flavonoids. Regarding their molecular structure, they present more than one aromatic ring, generally arranged as a diphenylpropane skeleton (C_6-C_3-C_6) in Figure 1.

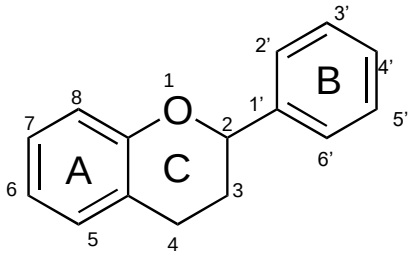

Figure 1- Diphenylpropane structure. Adapted from Literature (Panche et al., 2016).

The substitution pattern on the C-ring (Figure 1) can result in several flavonoids classes, such as flavones, flavonones, flavonols, flavanols, isoflavones, and anthocyanidins which have a different distribution in food products (Balasundram et al., 2006; Hollman & Katan, 1999). Besides that, substitutions in B-ring and/or A-ring (Figure 1) result in the different compounds within each class of flavonoids. These substitutions may occur through acylation, glycosylation, or oxygenation (Balasundram et al., 2006). On the other hand, the absence of the oxo group results in flavanols and anthocyanidins, these last ones, which are characterized to have an oxygen molecule with a positive charge in the diphenylpropane backbone. Regarding the presence of flavonoids in nature, flavonols and flavones are the major compounds in onions and tea, while vegetables are a reliable source of flavanones (Durazzo et al., 2019; Panche et al., 2016). Furthermore, isoflavones, which are polyphenols with estrogenic functions, are mainly found in soybeans (Krizova et al., 2019). On the other hand, berries present a high source of anthocyanidins (Mahdavi et al., 2016). Flavonoids have several biological effects when consumed. For instance, they can act as anti-allergic, anti-diabetic, anti-inflammatory, anti-oxidant, or cardioprotective agents (Ekalu & Habila, 2020). In Table 2, there are presented several subclasses of flavonoids and their biological activity.

Table 2- Flavonoids subclasses and different applications.

Subclass	Food sources and potential applications	References
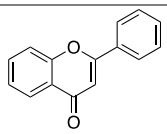 Flavone	Luteolin showed anti-cancer activity in simulated adenocarcinoma cells.	(Meng et al., 2016).
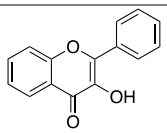 Flavonol	Quercetin showed prevention of age-related diseases.	(Bientinesi et al., 2022).
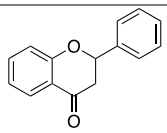 Flavonone	Hesperidin had protective activity against high glucose induced damage in diabetes.	(Liu et al., 2017).
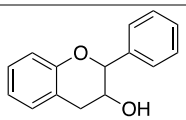 Flavanol	The intake of cocoa flavanols (epicatechin and catechin) can improve the cognitive function in elderly individuals.	(Mastroiacovo et al., 2015)
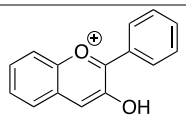 Anthocyanidin	The consumption of berry anthocyanidins (cyanidin, malvidin, peonidin, petudinin and delphinidin) can prevent recurrence of lung cancer.	(Kausar et al., 2012).
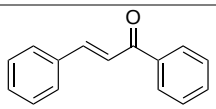 Chalcone	Lisochalcone A showed Anti-obesity activity and reduction of the synthesis of fatty acids.	(Liou et al., 2019)
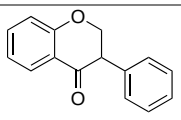 Isoflavonoid	Genistein has actively prevented postmenopausal symptoms.	(Thangavel et al., 2019)

The glycosylated form of anthocyanidins (anthocyanins) and their technological application, will be the focus of this dissertation. Thus, a detailed description of anthocyanins chemistry and bioactivity, will be presented.

2. Anthocyanins

Anthocyanins (ANCs) are derived from the Greek words *Anthos* and *kyanos which* means flower and blue, respectively. These flavonoids are naturally present in vascular plants, playing an important role in their reproduction, due to the intense colors that they possess leading to the attraction of pollinators (Winkel-Shirley, 2001). Since these molecules can produce such intense colors, they are capable of absorbing light at different wavelengths (Winkel-Shirley, 2001). Furthermore, the maximum wavelength absorption described in the literature is between 465 nm and 550 nm (visible light) and between 270 nm and 280 nm (UV-light), mainly due to the eight conjugated bonds and the positive charge in the chemical structure, consequently making ANCs highly colored under acidic conditions (Fernandes et al., 2020; He & Giusti, 2010). ANCs can present various colors, from red to orange and from violet to blue, mostly due to their chemical structure, based on the 2-phenylchromenylium (flavylium cation, Figure 2), having different substitution patterns such as hydroxylation, methylation, or acylation (Wrolstad et al., 2005). When a glycosylated group is not bonded to the main molecule, these are called anthocyanidins (Castañeda-Ovando et al., 2009). The most common forms of anthocyanidins and ANCs found in nature are presented in Table 3.

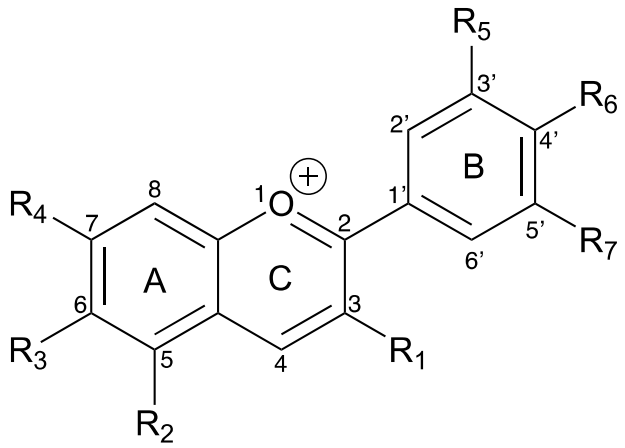

Figure 2- Flavylium cation generic chemical structure.

Table 3- Most common anthocyanidins found in natural sources.

Name	Substitution pattern							Distribution in nature[1]
	R_1	R_2	R_3	R_4	R_5	R_6	R_7	
Cyanidin	OH	OH	H	OH	H	OH	H	Berries, red onion, red cabbage
Delphinidin	OH	OH	H	OH	OH	OH	OH	Black currant, purple carrot
Pelargonidin	OH	OH	H	OH	H	OH	H	Strawberry, banana
Peonidin	OH	OH	H	OH	OMe	OH	H	Mango
Petunidin	OH	OH	H	OH	OMe	OH	OH	Bilberry, purple botato
Malvidin	OH	H	H	OH	OMe	OH	OMe	Bilberry and red grape

[1]: Adapted from literature (Brown, 2005; Bueno et al., 2012; Castañeda-Ovando et al., 2009; Durazzo et al., 2019).

The structural diversity of ANCs in nature is mainly caused by the substitution pattern in the flavylium cation, by hydroxyl or methoxyl groups, the number of sugars linked via glycosylated bonds in R1, the type of bond formed by those sugars and its position, the degree and type of esterification between aliphatic or aromatic acids that can be connected to the sugars (Bueno et al., 2012). The most common sugar units bonded to ANCs, via O-linkages, are glucose, galactose, rhamnose, xylose, and arabinose, as 3-glycosides or 3,5-diglycosides (Bueno et al., 2012). The main form of glycoside-derived forms found in nature are: 3-monosides, like cyanidin-3-O-glucoside (Cy3glc) which is the most common anthocyanin in nature (Kong et al., 2003); 3-biosides, such as cyanidin 3-(3",6"-dimalonylglucoside) and 3,5- and 3,7-diglucosides, such as cyanidin 3,5-diglucoside and malvidin 3,5-diglucoside (Figure 3) (Castañeda-Ovando et al., 2009; Fossen et al., 1996).

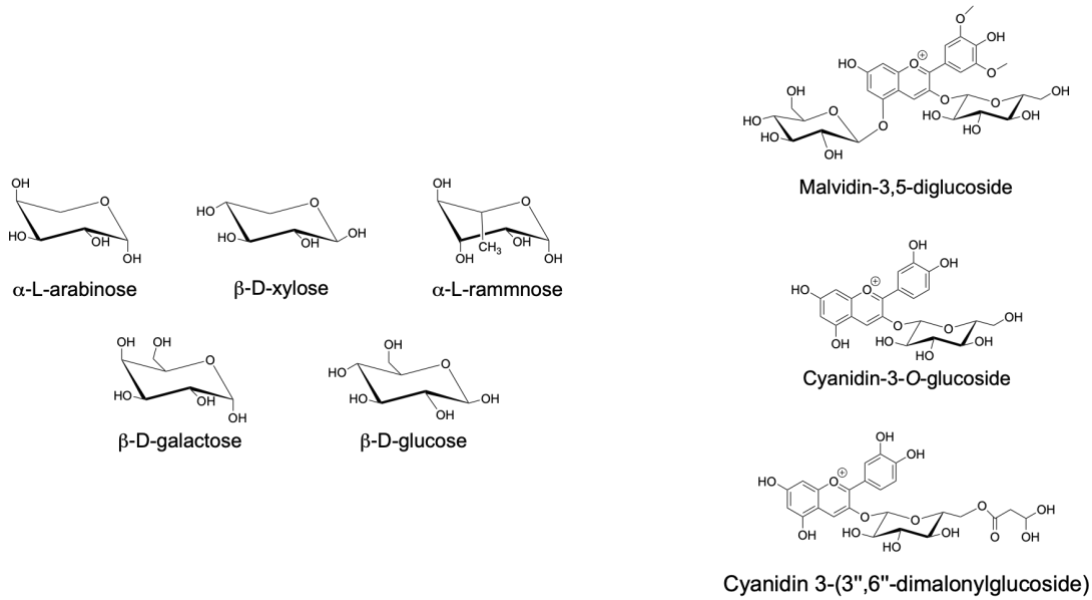

Figure 3- Sugars moieties and corresponding derivates of anthocyanins.

On the other hand, rutinose, sambubiose, and sophorose are the most common biosides that are linked in ANCs molecular structure (Bueno et al., 2012). It is important to be noticed that glycosylated anthocyanidins can have different stability depending on how the sugar unit is connected to the parent structure (Jordheim, 2007). Besides that, glycosylation can increase the water solubility of the original anthocyanidin (Bueno et al., 2012).

In addition to the linkage of sugars to ANCs, *O*-acylation can also appear in various molecules (Bueno et al., 2012). *O*-acylation happens when organic acids are bonded to sugar moieties. Examples of acylating agents are the p-coumaric acid, caffeic acid (hydroxycinnamic acids), gallic acid (hydroxybenzoic acid), acetic acid, oxalic acid, and succinic acid (aliphatic acids) (Figure 4**)** (Bueno et al., 2012). In general, acylation can improve anthocyanin stability, more specifically, when occurs at C_3 and C_5 since it can hinder enzyme activity by a large number of ligands present in the flavylium cation skeleton (Rodriguez-Saona et al., 1999). On the other hand, a high degree of acylation can have an impact on the adsorption of ANCs on the gastrointestinal tract (Prior & Wu, 2006).

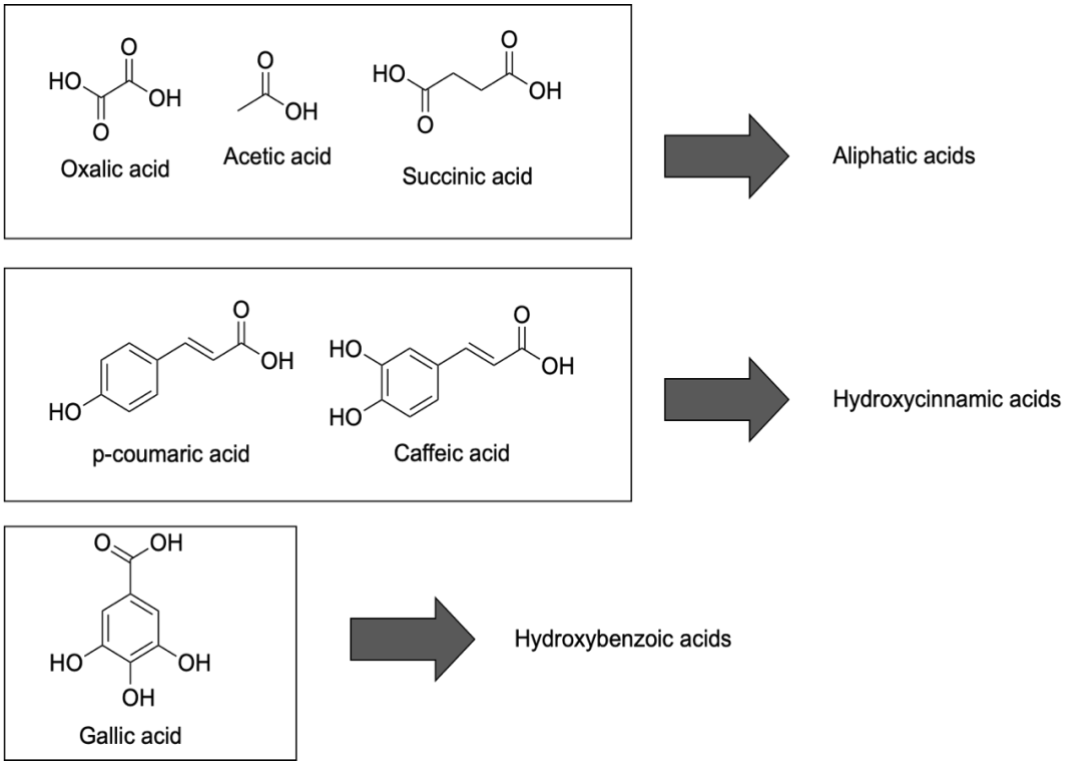

Figure 4- Examples of organic acids that can be bonded to anthocyanins by acylation.

In general, the fact that ANCs can suffer glycosylation, acylation, and methylation with other molecules, provides a large number of derivates of simple anthocyanidins, that can appear as polymerized units or not (Prior & Wu, 2006). This can be useful to find new structures that are naturally stable by these phenomena and provide a different range of colors. Besides that, this type of reactions can be regulated by genetic factors or external factors that can damage the plant and decrease the stability of these pigments, such as light, pH, and temperature. Nevertheless, this type of substitution in the aglycone backbone can increase the stability of ANCs to aggressive conditions (Prior & Wu, 2006).

2.1. Stability of anthocyanins: influence of the pH and temperature

Temperature, complexity of the ANCs structure, pH, presence of oxygen, light, enzyme activity, other flavonoids, and metallic ions are examples of factors that can severely affect ANCs stability (Castañeda-Ovando et al., 2009; Ersus & Yurdagel, 2007). These conditions make extraction of ANCs relatively challenging and are determinant on the stability of these pigments prior extraction.

The pH is one of the main elements affecting ANCs stability and chemical reactivity, being the main reason why ANCs are highly unstable in the isolated form. At acidic pH, the

flavylium cation, presents a strong red color. When the pH increase, two reactions occur: (i) the flavylium cation (Figure 5, AH+) rapidly transforms into a quinoidal base (Figure 5, A), (ii) the flavylium cation transforms into a carbinol pseudobase (Figure 5, B). These reactions occur simultaneously, and the deprotonation of the flavylium cation occurs more rapidly than the hydration, however, the formation of the hemiketal form is thermodynamically more stable (Brouillard & Dubois, 1977; Cruz et al., 2015). Then, the hemiketal can undergo a reaction of tautomerization, that occurs in sub seconds, forming the *cis*-chalcone form (Figure 5, Cc), being further isomerized into the *trans*-chalcone form (Figure 5, Ct) (Brouillard & Dubois, 1977; Cruz et al., 2015). It is important to notice that this system of equilibrium is pH reversed, *i.e* the flavylium cation can be obtained by reacidification of the solution.

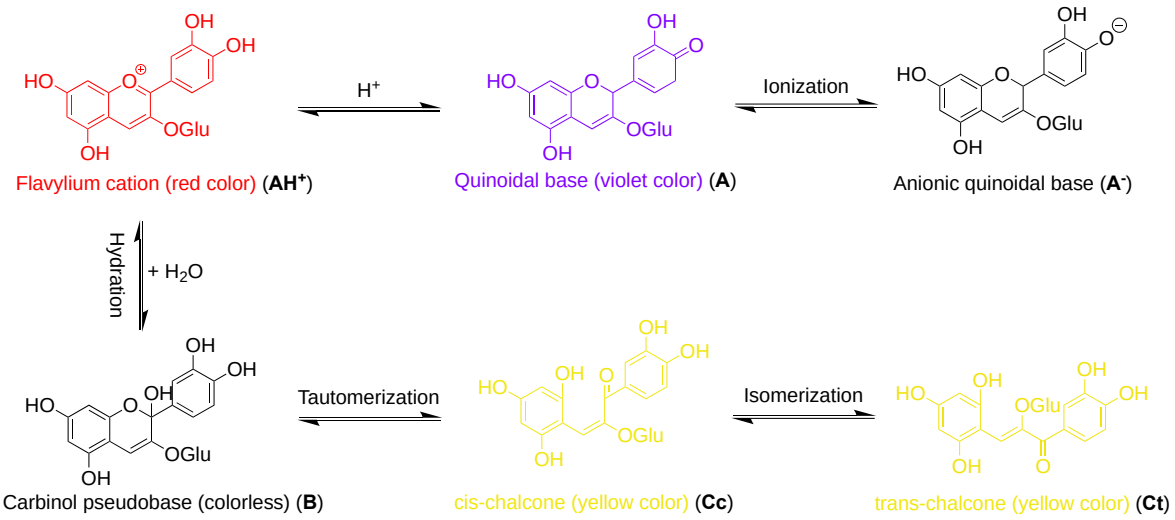

Figure 5- Acid-base equilibrium of Cyanidin-3-*O*-glucoside. Adapted from (Brouillard, 1982; Bueno et al., 2012).

The thermal degradation of ANCs is another problem that the food industry faces when processing food that contains these pigments. Thermal degradation may follow a first-order kinetic process (Andersen & Jordheim, 2013). Besides that, temperature effect on ANCs is directly influenced by the type of raw material used, the pH and co-pigments that may be present in the extracted matrix (Oancea, 2021). On the other hand, acylation and methoxylation can enhance ANCs stability at higher temperatures (Shahidi, 2012). Despite this, ANCs can undergo different changes in the chemical structure. For instance, the elevated temperatures can shift the ANCs equilibrium (Figure 5) to the formation of the tautomeric open-form (Cc), that can happen more frequently in monoglycosidic ANCs, such as Cy3glc(Shahidi, 2012). Despite the noticeable sensibility to heat by ANCs, there are several methods that can be applied that can decrease it. For example, the addition of sugars can promote more hydrogen bonds interactions, therefore decreasing the

susceptibly to heat. The encapsulation with proteins, gums or cyclodextrins by electrostatic forces, hydrogen bonds or ionic interactions, results in stable complexes that can decrease ANCs hydrolysis (Oancea, 2021).

2.2. Bioactivity of anthocyanins

ANCs have been studied as nutraceuticals, with potential in decreasing the incidence of chronic diseases (Oz, 2017). Specifically, red wine consumption have been showed to decrease coronary heart diseases, in a study involving individuals in France (Renaud & de Lorgeril, 1992). Consequently, several studies have been published to demonstrate the potential health benefits of several classes of polyphenols. *In vitro* models showed that ANCs have a high antioxidant activity, being responsible to eliminate free radicals in the organism and cease the chain reaction of overproduction of reactive oxygen species that can cause oxidative damage in tissues and cells, leading to inflammation and many cardiovascular diseases (He & Giusti, 2010). Based on this, a mulberry extract was studied to investigate the protection against oxidative stress induced by H_2O_2 in an immortal human liver hepatoma cell line (HepG2) (Yan et al., 2017). It was suggested that this extract could mitigate oxidative stress by activating the mitogen-activated protein kinases that phosphorylates the serine and threonine residues in the nuclear factor erythroid 2-related factor 2 (Sun et al., 2009). This pathway acts an defense mechanism in cells by producing antioxidant enzymes (Yan et al., 2017). Another potential effect that ANCs could have in the human body is the prevention of obesity. A recent study showed that the application of an ANC-rich extract from black currant on mice, could reduce weight and maintain a healthy gut microbiome (Esposito et al., 2015). ANCs were also suggested as potential compounds that can prevent diabetes. Cyanidin-3-*O*-glucoside extracted from mulberry fruits, was investigated as a new protective compound against induced apoptosis in a model of pancreatic cells (Lee et al., 2015). The authors demonstrated that Cyanidin-3-*O*-glucoside can scavenge free radical oxygen species, inhibit lipid oxidation and reduce apoptotic cell rate (Lee et al., 2015). A resume of these biological properties of ANCs is presented in Figure 6.

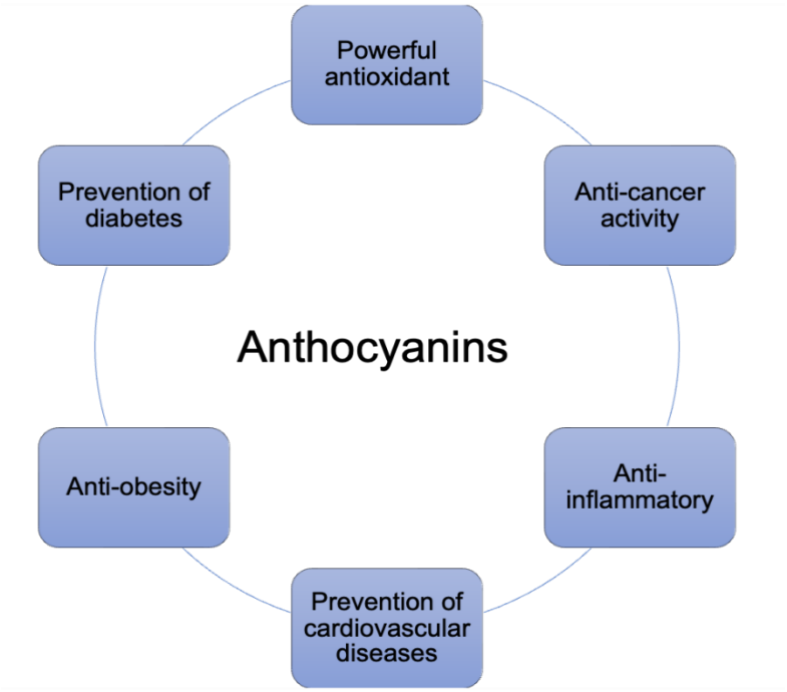

Figure 6- Relevant potential biological activities of anthocyanins when consumed.

2.3. Anthocyanins in the food industry: the improvement of organoleptic properties

ANCs are one of the most consumed flavonoids in the human diet since they can naturally be found in food and herbal medicines that, for example, use berries and seeds (Bueno et al., 2012). These flavonoids are commonly ingested in the form of fruits, products derived from fruits (red wine, jams or fruit juices) and some vegetables and grains (eggplant, red cabbage or black rice) (Krga & Milenkovic, 2019). ANCs extraction from natural sources may present some challenges and are highly unstable. However, some food products are being fortified with these pigments, with different applications and using different extractions techniques (Echegaray et al., 2020). This can be beneficial since it can improve the organoleptic properties of food and its overall functional potential. In general, most of its applications comes from the use of waste from several vegetables' sources, such as fruit skins or grapes marc.

A study showed that Kefir, a fermented lactic product, fortified with ANCs from grape skins (7 mg per 100 mL of Kefir), obtained by enzymatic extraction and further lyophilization, formed a red colored Kefir without the addition of synthetic dyes (Montibeller et al., 2018). Additionally, around 67% of the total ANCs were still in the yogurt after 16 days of storage at 7ºC in the absence of light.

In another study, a blueberry powder rich in Cy3glc was added to a yogurt, generating a more appealing product, with higher phenolic content and a relatively high shelf-life, holding its color for 2 months (Wallace & Giusti, 2008).

In an earlier study, purple-fleshed sweet potato extract was proposed as a new source of natural colorants for the food industry (Quan et al., 2019). For this, the kinetic of pigment degradation of a purple-fleshed sweet potato extract was evaluated in three different storages conditions: 25ºC with the absence of light, 37ºC with the absence of light and 25ºC with fluorescent light (Quan et al., 2019). The results showed that the degradation of ANCs was 88%, both for the samples without light exposure and storage temperature of 37ºC as well as the samples that were exposed to 25ºC by fluorescent light (Quan et al., 2019). However, ANCs degradation at 25ºC with the absence of light was around 51% in the same interval of time. Additionally, results showed that peonidin caffeoyl-feruloyl sophoroside-5-*O*-glucoside was the most stable anthocyanin along the study performed, which can be explained by the high degree of acylation, providing hydrophobic and π-π interactions that can increase its stability (Quan et al., 2019).

Another relevant result showed in this study is the noticeable change in the ΔEab, which is an indicator on how the color is precepted. This value is typically used when measuring color in the CIELAB color space and reflects whether the obtained color differences can be noticeable by the human-eye. After 6 months of storage, samples stored at room temperature had noticeable changes in this value. However, the value was much higher compared to when samples were kept at 37ºC (no light) and room temperature (fluorescent light). In fact, after 6 months of storage, the color change was more noticeable when samples were kept in fluorescent light than at high storage temperatures (Quan et al., 2019). This type of extract could be improved to function as new food colorant, controlling the exposure of light, and maintaining a low temperature during storage.

2.4. General methods for anthocyanins stabilization

The instability of ANCs can be noticed during the production of a specific food product and its storage, having a major impact in the organoleptic properties and nutritional value of products that contains ANCs. For this reason, food scientists are focused on solving this problem, improving ANCs based products stability under the production and storage conditions used in the food industry. To achieve ANCs stabilization, several methods have been developed and can be divided in two categories 1) ANCs stabilization increasing their resistance to severe conditions; 2) the use of different molecules to protect or decrease the severance of degradation by external factors (Huang et al., 2021). These methods are represented in a form of diagram, in Figure 7.

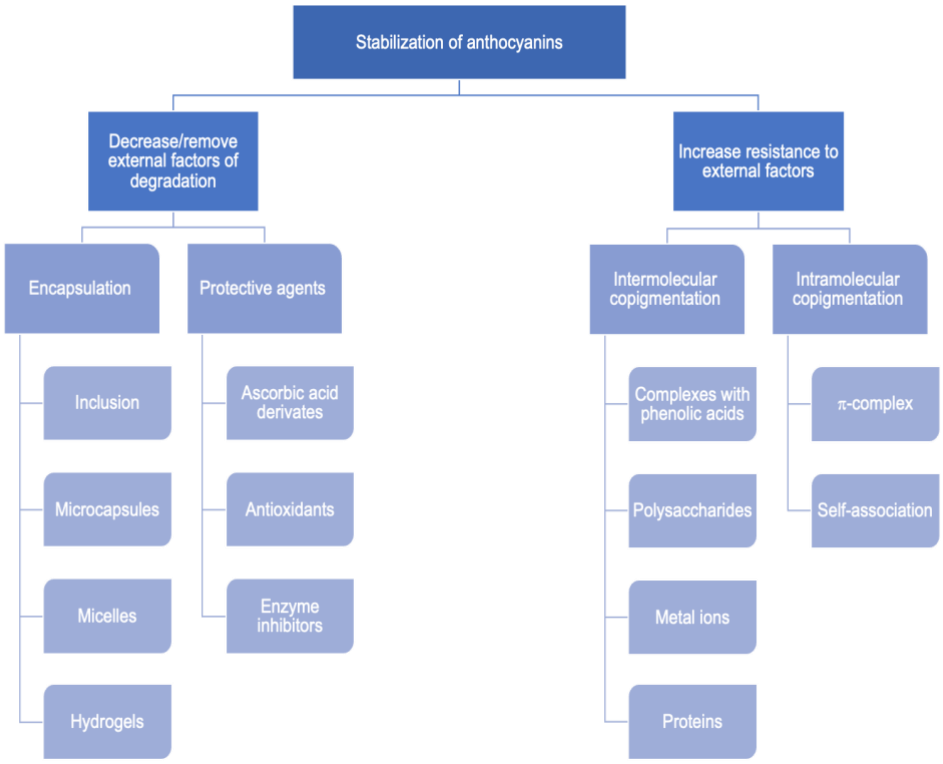

Figure 7- Diagram representing several methods of stabilization of anthocyanins.

The protection of ANCs can be achieved by phenomenon's of copigmentation, that occurs when a copigment interacts with the chromophore of ANCs by non-covalent interactions. Copigmentation can be being divided in intermolecular and intramolecular copigmentation. Intermolecular copigmentation can happen when: 1) two similar ANCs molecules interact with each other; 2) interaction of different ANCs structures; 3) a non-anthocyanic compound (phenolic compounds, organic acids, proteins, or metallic ions) interact with an ANC molecule, by ionic interactions, Van der Waals forces, hydrogen bonds or hydrophobic interactions (Trouillas et al., 2016). Furthermore, the first two situations are commonly named as self-association, made possible by π-π interaction between hydrophobic aromatic moieties in both ANCs (Huang et al., 2021). Copigmentation is usually considered a method based on the protection of sensible moieties of ANCs, giving steric hindrance against molecules that can degrade ANCs (Huang et al., 2021). Furthermore, it can be detected by a hyperchromic shift and a bathochromic shift (increase of the maximum wavelength). When purple sweet potato ANCs were copigmented with tannic acid at 0.02 M, an increase of the color intensity of ANCs could be observed (Susanti et al., 2018). However, bathochromic shifts can be a disadvantage since the original color of the pigment isolated can be modified.

Several methods that can protect ANCs molecules have showed different applications in terms of encapsulation. For example, inclusion of Cy3glc was studied using β-cyclodextrin,

forming non-covalent interactions with ANCs (Fernandes et al., 2018). Results showed that the inclusion was successful in protecting ANCs against thermal degradation.

Other stabilization method is the application of solid lipid nanoparticles (SLNs), that are based on the formation of colloidal transporters of unstable molecules, being solid at room temperature and at human body temperatures (Borges et al., 2020). These transporters are generally made of lipids and are dispersed in a aqueous solution and stabilized by a surfactant molecule, that cover the lipid core (Borges et al., 2020). The application of SLNs was studied in the stabilization of ANCs (Ravanfar et al., 2016). The SLNs were based on the use of egg lecithin, Span 85 (a natural surfactant based on oleic acid) and palmitic acid. Results showed that the microencapsulation was successful, with approximately 90% of ANCs entrapment and these SLNs showed better stability compared to the free pigments, specially at elevated temperatures (Ravanfar et al., 2016). Despite the apparent success on the application of SLNs, there are a few disadvantages when applying this method in ANCs. These pigments have a hydrophilic nature, which results in a higher tendency of partition into the aqueous phase during the formation of SLNs (Ravanfar et al., 2016). Besides that, lipid crystals can suffer recrystallization, lowering the loading efficiency (Zhai & Zhai, 2014).

Another alternative proposed is the interaction between proteins and ANCs. This interaction is usually promoted by Van der Waals bonds or hydrogen bridge bonds. A recent study tested the interaction between ovalbumin and Cy3glc (Fu et al., 2020). For this, the authors tested the formation of ANCs complexed with ovalbumin at acidic pH (pH= 2.4) and neutral pH (pH=7.1). Results showed that at acidic pH, the particle size of ovalbumin and the complexes formed by it, were smaller compared to neutral pH, which may indicate that the acidic pH can have influence on the aggregation of the protein molecule (Fu et al., 2020). Besides that, it was noticeable a higher thermostability in both pH's of these protein-ANCs complexes (Fu et al., 2020). However, binding affinity of ovalbumin and Cy3glc was higher in neutral pH, which restricts the use of these complexes in foods that require acidic pH, such as, dairy products or fruit juices.

The use of protective agents such as ascorbic acid derivates can remove external factors that degrade anthocyanins, serving a different purpose as the other methods mentioned before. Ascorbic acid derivates, such as L-ascorbic acid 2-phosphate sesquimagnesium salt hydrate, not only had a protective effect in ANCs, bleaching them in a lower degree compared to ascorbic acid, but also served as a source of vitamin C (Gérard et al., 2019)

Encapsulation of ANCs using polyethylene glycol and chitosan as wall materials was studied (Fang et al., 2020). Polyethylene glycol is a macromolecular polymer that present

low toxicity, hydrophilic properties, and biocompatibility, while chitosan is a biopolymer insoluble in water, high level of absorption and is biodegradable. To perform this stabilization, it was used the emulsion-congealing technology, based on the sensibility of polyethylene glycol to temperature changes, resulting in the encapsulation of ANCs (Fang et al., 2020). In this study, ANCs were extracted from mulberries. Results showed that the storage of encapsulated ANCs during 12 months at 25ºC, resulted in a slower decrease in the antioxidant activity, compared to free ANCs (Fang et al., 2020).

3. Polyelectrolyte complexes polysaccharide based interacting systems

A more recent approach for ANCs stabilization consists of its incorporation on polyelectrolyte complexes (PECs). PECs are macromolecular complexes, that are formed when two oppositely charged molecules interact, forming a polymeric chain (Meka et al., 2017). The formation of these complexes can be accomplished by adding a polyelectrolyte solution into another polyelectrolyte solution under constant stirring (Meka et al., 2017). Chemically, the formation of these complexes involve three steps: the primary complex is formed after mixing the two oppositely charged molecules; then, an intermediate complex forms by electrostatic bonds that create a polymeric chain; finally, occurs aggregation of the intermediate complexes by hydrophobic interactions (Meka et al., 2017; Thünemann et al., 2004). These reactions are represented in Figure 8. It is important to notice that the conditions used in the formation of PECs, such as pH, salt, charge distribution, mixing ratio (duration and intensity), type of ionic groups, temperature and molecular weight can change the morphology, function and yield of PECs (Meka et al., 2017).

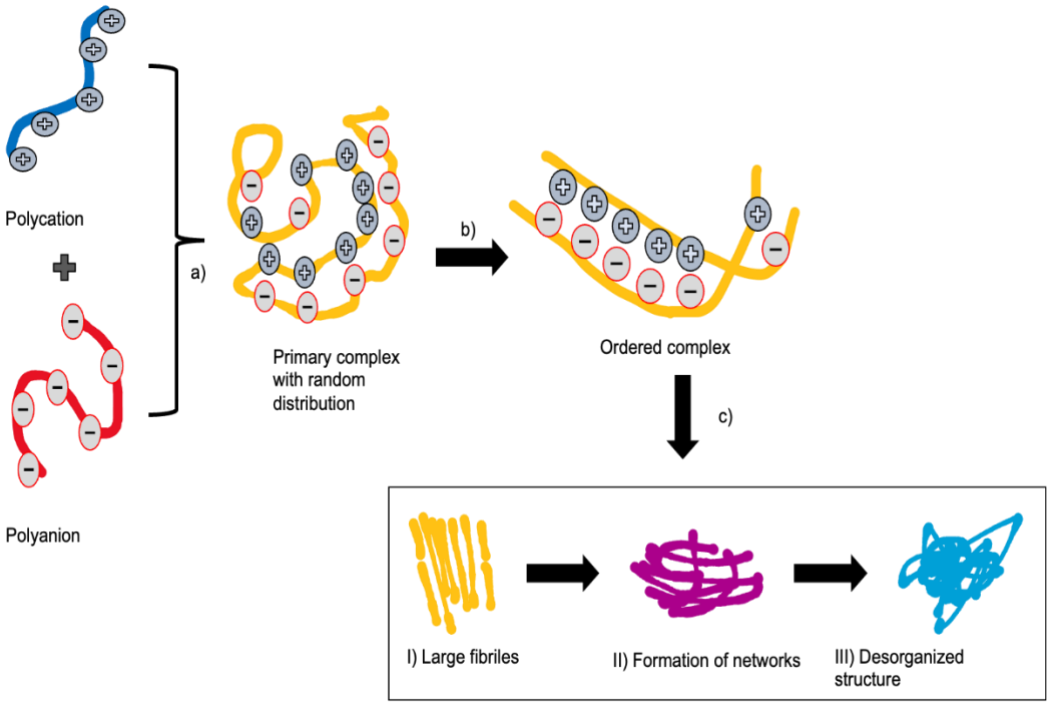

Figure 8- Representation of the formation of polyelectrolyte complexes. a) A primary complex is formed immediately after the addition of the polyanion to the polycation; b) The polyelectrolyte complex acquires an ordered distribution, by establishing new electrostatic bonds. This process can take about two hours. c) The ordered complex becomes more aggregated, by hydrophobic bonds, transforming this complex insoluble in most solvents due to its structure. Adapted from literature (Meka et al., 2017).

Based on their structure, PECs can be divided into two categories,: (i) stoichiometric complexes, where two oppositely charged polyelectrolytes are mixed in a 1:1 charge ratio, and are mutually neutralized, precipitating in solution (Shchipunov & Postnova, 2009; Shovsky et al., 2009). These types of PECs can be used to produce membrane materials, coatings and binders in large-scale processes (Ji et al., 2010; Li et al., 2016; Shchipunov & Postnova, 2009). (ii) non-stoichiometric complexes, where two polyelectrolytes are mixed in different charge ratios. In contrast to stoichiometric complexes, these type of systems can be applied in drug delivery systems and encapsulation of bioactive compounds in food systems (Shchipunov & Postnova, 2009).

Another classification can be made, based on the main interactions acting during PECs formation. Two-phase system complexes can present a high level of aggregation (insoluble complexes) with several polyelectrolyte chains, that are stabilized by a polycation or polyanion in excess, that is on the surface of the complex (Shchipunov & Postnova, 2009). These precipitates are formed when polyanions and polycations interact with each other, resulting in a polymer-rich phase and a diluted phase. When the polymer-rich phase achieves thermodynamic equilibrium, it acquires properties of an liquid elastic, composed of two oppositely charged PECs species and rearrangement of ions pairs between different

polymers (Rumyantsev et al., 2021). Additionally, the hydrophobicity character of these type of PECs enhances this precipitation, that can be repeated by continuous washing and drying of the complex solution (Shchipunov & Postnova, 2009). The electrostatic interactions that are responsible for the complexation, makes these complexes very stable, mostly due to their tendency to form highly associated molecules.

On the other hand, water soluble complexes, only occur when: i) one of the components have weak ionic groups; ii) when one of the two polymers has a long-chain structure; iii) there are significant differences of molecular weights between the polymers used; iv) a specific concentration of salt must be used. These types of complexes assume a molecular conformation similar to a ladder structure (Buriuli & Verma, 2017).

Finally, colloidally stable PECs are colloidal systems that differ between each other depending on the compatibility between polyelectrolytes. When compatible charges densities interact, compact colloidal structures are formed, while when the charge is not compatible, colloidal particles with high swelling ability occur (Buriuli & Verma, 2017).

Examples of application of these PECs systems are presented in Table 4.

Table 4- Several applications in the literature of the production of PECs.

Main application	Polycation	Polyanion	Type of PEC's	Reference
Drug delivery of curcumin	Chitosan	Dextran sulfate	Two-phase system	(Anitha et al., 2011)
Gene delivery	Polyethylenimine	Plasmid DNA	Colloidal complex	(Zaitsev et al., 2004)
Improvement of anthocyanins bioaccessibility	Chitosan	Pectin	Two-phase system	(Sarkar et al., 2021)
Encapsulation of assai pulp oil	Chitosan	Alginate	Two-phase system	(Teixeira-Costa et al., 2020)

Despite the wide application of PECs, there are a few disadvantages. For example, salt ions have a negative impact in PECs formation, since it can reduce the interaction between PECs molecules and can determinate the rearrangement of these complexes (Meka et al., 2017). Other limitation is related to the low adsorbing properties and a relatively low success on measuring the amount of complexed polymers (Meka et al., 2017).

One of the most used polyelectrolytes are polysaccharides with a polymerized molecular structure. They can be obtained from plants, fruits, and marine sources. From seafood shells, it can be extracted chitosan, a water soluble biopolymer, (a N-deacetylated derivate of chitin), that has positive charge, making it extremely versatile in terms of their application (Hamed et al., 2016). The chemical structure of chitosan is based on α (1→4) 2-amino-2-deoxy-β-D-glucan repeated structures. It has low toxicity, and it is biodegradable (Bellich et al., 2016). Another biopolymer that can be applied in PECs systems is pectin, that can be found in fruits, such as apple pomace, and is an anionic polysaccharide of several (1→4)-α-D-galacturonic acid monomers. Pectin is generally used as a stabilizer in the food industry, as a thickening agent or gelling agent in dairy products and fruit jams (Mohamed et al., 2020). Alginate is a biopolymer extracted from brown algae, that can form gels by the addition of polyvalent ions, such as calcium, producing a strong insoluble polymer that can be used in foods, to increase shelf life by the formation of a water barrier, preservation of flavor and inhibition of lipid oxidation (Song et al., 2011). Alginates are composed by units of 1,4-β-d-mannuronic and α-L-guluronic acids at different ratios, and different sequences of 1-4 bonds in the polymer chain. The use of these of biopolymers as PECs systems have been explored in several studies, for example: formulation of calcium alginate gels as a carrier of polymyxin B for controlled release in the vaginal tract (Ferreira et al., 2017);

Pectin-gelatin PECs as a system delivery of curcumin (Shih et al., 2018); Production of chitosan-xanthum gum PECs as a delivery system of ibuprofen (Ćirić et al., 2020); κ-carrageenan-chitosan PECs for a controlled release system, by intranasal application, of sumatriptan succinate (Alavi & Mortazavi, 2018).

3.1. PECs systems as a new mechanism of stabilization of anthocyanins

ANCs association with biopolymers, such as polysaccharides, or using PECs, may also provide their stabilization (Cavalcanti et al., 2011; Jeong & Na, 2012). In a recent study, different combinations of pectin and chitosan in the presence of $CaCl_2$, allowed the encapsulation of ANCs extracted from *Carissa carandas*, by forming insoluble PECs (Sarkar et al., 2021). Results shown that ANCs and water molecules were entrapped into the complex network. Furthermore, formulation containing pectin at 60 $mgmL^{-1}$ and chitosan at 7 $mgmL^{-1}$ had a higher bioaccessibility of ANCs, at 24.3% (Sarkar et al., 2021). Another study showed the potential application of the formation of PECs complex coacervates, by encapsulating ANCs, in this case, using gum arabic and gelatin as wall materials for the encapsulation of black raspberry ANCs (Shaddel et al., 2018). According to the results, a weight ratio of gelatin: gum arabic: black raspberry ANCs (1:1:1) with a concentration of 0,075 $g.mL^{-1}$ showed a high encapsulation efficiency, high loading capacity, retention of ANCs and red color retention (Shaddel et al., 2018).

Incorporation of ANCs into a nanocarrier system can be made by the interaction of flavylium cations with negatively charged molecules, such as natural polysaccharides. Dextran sulfate, a negatively charged polyssacharide, was used to form PECs with flavylium cations from a crude bilberry extract (Klimaviciute et al., 2015). This polyssacharide was used since it was expected that the presence of strong negative sulfate groups in dextran suflate, would adsorb ANCs in a flavylium cation form. The results showed that this interaction caused hyperchromic shift and hypsochromic shift in the spectrum of the complex. Additionally, it was observed that the total concentration and weight ratio had significant impact on the formation of nanoparticles of dextran sulfate/ANCs (Klimaviciute et al., 2015).

Chondroitin sulfate and ANCs interaction was studied as a new mechanism to enhance ANCs stabilization (Jeong & Na, 2012). Results showed that a charge complex was formed during intermolecular stacking, via $\pi-\pi$ interactions between ANCs molecules, and ionic interactions due to the negatively charged sulfate groups and positively charged flavylium cations, which resulted in a relatively stable nanocomplex (Jeong & Na, 2012). Besides that, the charged complex showed higher free radical scavenging than the free ANCs, since it

protected ANCs moieties from hydration, and a significantly higher *in vitro* anti-oxidant activity in HeLa cells comparing to free ANCs (Jeong & Na, 2012). Another relevant approach was made by combining carrageenan with a ANCs rich extract from bilberries (Navikaite et al., 2016). Two types of carrageenan were tested, ι-carrageenan and κ-carrageenan, which differ from each other in the number of sulfate groups, since ι-carrageenan has two sulfate groups and κ-carrageenan has only one (Navikaite et al., 2016). It was shown that the nanocomplexes were only formed by charge-charge interactions and precipitated into solution due to the formation of PECs (Navikaite et al., 2016). Besides that, these nanocomplexes were dependent on the total concentration of the reagents and the ratio of ANCs and carrageenan molecules (Navikaite et al., 2016). When carrageenan molecules interact with ANCs, it forms complexes due to the interaction of sulfate groups and the flavylium cation, as reported in the literature (Navikaite et al., 2016).

The carrageenan (CRG) is a mucopolysaccharide presented in cell walls of red seaweed species like *Chondrus crispus*, *Eucheuma denticulatum* and *Kappaphycus alverezii* (Martín-Del-Campo et al., 2021; Necas & Bartosikova, 2013). Different species have different compositions of CRG. For instance, the main composition of *Chondrus crispus* is κ- and λ-CRG, while *Eucheuma denticulatum* has mainly ι-CRG in its composition (McHugh, 2003). Regarding its chemical structure, it is a sulfated polygalactan, with alternative units of D-galactose and 3,6-anhydro-galactose linked by a α-1,3 and β-1,4-glycosidic bond (Necas & Bartosikova, 2013). The CRG powder is typically used in the food industry as a thickener in the dairy industry, or as natural substitute of gelatin (McHugh, 2003). This biopolymer have shown potential as forming different complexes with oppositely charged molecules (drugs or other biopolymers), with application as a control release system of drugs or other sensitive bioactive compounds (Pacheco-Quito et al., 2020). Giving polyelectrolytes potential to overcome some of ANCs technological limitations, the main objective of this project was to produce and characterize PECs systems with λ-CRG and ANCs extracted from blackberries. This type of stabilization was used since it can be regarded to a green process, without the use of any organic solvent, at a room temperature and without any significant consumption of energy. Furthermore, these systems form soluble or insoluble complexes, however, the main focus is the insoluble complexes, that can be achieved by manipulating the concentration of each component, the charge ratio, the ionic strength of the medium and the weight ratio (Klimaviciute et al., 2015).The ANCs were extracted from blackberries by-products due to its high concentration on monoglucoside ANCs and easily obtainment. λ-CRG was used due to the fact that previous studies reported that others types of CRG (κ- and ι-) had a potential to interact with positively charged molecules, polymers

or drugs, and form ionic interactions with ANCs. (Li et al., 2014). Besides that, the insertion of an additional sulfate group, could provoke a stronger electrostatic interaction with flavylium cations.

Experimental design

The need to replace synthetic additives in the food industry by their natural counterparts, led to increasing research on natural-based food colorants, including new sources, extraction methodologies and stabilization mechanisms for proper technological performance. Therefore, the main objective of this project was to produce a new food ingredient by the electrostatic complexation of a blackberry anthocyanic extract, with a sulfated polysaccharide, followed by a detailed physicochemical characterization of these complexes. The present work was divided in four main steps, summarized in Figure 9.

a) Extraction and purification of anthocyanins from blackberries. Physicochemical and bioactivity characterization of the anthocyanin-rich extract: Folin-Ciocalteau for the determination of the total phenolic content; HPLC-DAD/ESI-MS for anthocyanins and low molecular weight phenolic compounds quantification and identification, DPPH for antiradical activity; FRAP for antioxidant capacity; Protein quantification by Bradford method.
b) Studies of the optimal conditions for the complexation between anthocyanins and λ-carrageenan by coacervation, using turbidimetry assays and the measurement of the zeta potential.
c) Physicochemical characterization of the produced insoluble complexes. FTIR-ATR SEM and cryo-SEM for structural and morphology elucidation; DSC/TGA to evaluate the thermal stability and anthocyanins release pattern in different experimental conditions.

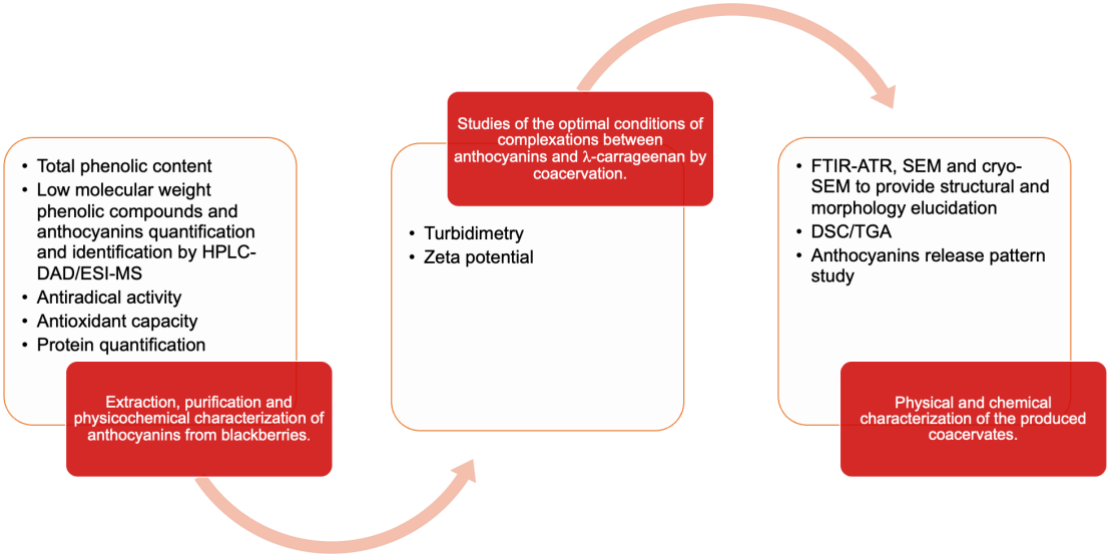

Figure 9- Schematic representation of the process used to produce insoluble complexes from a blackberry extract.

Materials and methods

1. Materials

All reagents used were of analytical grade or superior. From Chem-Lab® (USA), 2,4,6-Tris(2-pyridyl)-s-triazine (TPTZ) acetic acid, acetonitrile, methanol (MeOH; CH_3OH) and sodium hydroxide was used. C-18 silica gel was obtained from Fluka®. From Sigma-Aldrich® (Spain), 2,2-diphenyl-1-picrylhydrazyl (DPPH), 4-morpholineethanesulfonic acid, 2-(N-morpholino) ethanesulfonic acid (MES), Bradford reagent, citric acid monohydrate, ethyl acetate, Folin-Ciocalteu reagent, λ-carrageenan (λ-CRG), sodium acetate trihydrate and sodium phosphate dibasic dihydrate were acquired. Hydrochloric acid was used from Honeywell® (USA). Phosphate saline buffer tablets (PBS), sodium carbonate was obtained from Pancreac AppliChem®. Purified water, produced by a Milli-Q filtration system was used for the preparation of all solutions.

2. Blackberry anthocyanins extraction and purification

Frozen blackberries were used to extract ANCs. Into a large beaker, blackberries (≈ 70 g) were macerated with 700 mL of acidified deionized water (HCl 2 %). The blackberries were crushed and kept stirring for 4 hours at room temperature (20 ºC). After this period, the solution was filtered on a porous tissue and the solid fraction, containing the vegetal residues, and these residues were subjected to a second solid-liquid extraction for 22 hours at room temperature (20 ºC). The raw extract was centrifuged at 10000 rpm for 10 min at 20 °C and purified in a Büchner funnel with a reverse phase C18 silica gel. After C18 gel pre-conditioning with methanol, the anthocyanic rich extract was applied and eluted with acidulated deionized water (HCl 2 %), to remove simple sugars, salts, organic acids, and other impurities that the extract may have. The anthocyanic fraction was recovered with acidified MeOH (HCl 2 %). Lastly, using a rotary evaporator, under vacuum at 35ºC, MeOH was evaporated, and the final product was redissolved in distilled water, freeze-dried, and kept at -20 ºC until further use.

3. Chemical characterization of blackberry anthocyanic extract

3.1. Determination of total phenolic content

The total phenolic content present in the blackberry extract was determined following the Folin-Ciocalteau method (Singleton & Rossi, 1965). The phenolic compounds present in the extract have the potential to reduce the mixture of phosphotungsten and phosphomolybdenum acids into blue colored oxides of tungsten and molybdenum. The reaction occurs in alkaline medium, and the coloration obtained shows a maximum at 750 nm, and its intensity is proportionately related to the concentration of phenolic compounds.

The samples were prepared in triplicates. 15 μL of blackberry anthocyanic extract at 1 mg. mL^{-1} was added into a 2000 μL eppendorf tube, followed by 75 μL of Folin-Ciocalteu reagent. Then, 500 μL of distilled water was added, and the tube was thoroughly mixed. To the Eppendorf tube, 300 μL of Na_2CO_3 at 20 % and 610 μL of distilled water was added, and the mixture was mixed again. The samples were allowed to stand in a dark place for 30 min. The blank was prepared as described before; however distilled water was used instead of the sample solution. To perform the assay, 350 μL was removed from the sample tube and blank tube to a 96-well plate, using a plate reader (PowerWave XS, Bio-TEK). The absorbance was measured at 750 nm. The total phenolic content was represented as μg equivalents of gallic acid / mg of extract (μg GAE / mg extract) using a calibration curve of gallic acid.

3.2. Protein quantification

The protein content was evaluated accordingly with the Bradford assay, as described elsewhere (Bradford, 1976). Briefly, 100 μL of the blackberry anthocyanic extract, prepared at 0.5 $mg.mL^{-1}$, was added to 200 μL of Bradford's reagent, corresponding to the sample solution. For the blank preparation, the extract was replaced by distilled water. Additionally, a control was made possible by the addition of 100 μL of extract and 200 μL of distilled water. The plate was left at room temperature in a dark environment for 10 minutes and the absorbance was measured at 595 nm in a plate reader (PowerWave XS, Bio-TEK). The results were expressed as mg equivalents of serum bovine albumin per mg of extract (μg BSAE / mg extract), using a calibration curve of serum bovine albumin.

3.3. Antiradical activity

To evaluate the antiradical capacity of the blackberry anthocyanic extract, an assay made with 2,2-diphenil-1-pycrilhydrazil radical (DPPH·) was performed. The DPPH is a free radical specie, that can be reduced by antioxidants present in the extract. The decrease of DPPH radicals can be noticed by measuring the absorbance at 515 nm. Briefly, three solutions were prepared, a blank sample (with distilled water and anthocyanic extract), a control sample (with DPPH and distilled water) and the sample (with DPPH and anthocyanic extract, prepared at 1 mg. mL^{-1}). The DPPH solution was prepared at 60 μM, by dissolving it in MeOH. The solutions were made in quadruplicates. Absorbance is measured at 515 nm in a plate reader (PowerWave XS, Bio-TEK) at 0 min, 5 min, 10 min, 15 min and 20 min. Results were expressed as μM equivalents of Trolox, using a calibration curve of Trolox.

3.4. Reducing capacity

The evaluation of the antioxidant capacity was made by the reduction of a complex of $[Fe(III)\text{-}TPTZ_2]^{3+}$ to $[Fe(II)\text{-}TPTZ_2]^{2+}$, at pH 3.6, due to the antioxidants present in the blackberry anthocyanic extract. The product of the reaction is detected by UV-Vis spectrophotometry, at 593 nm, since the maximum absorbance is recorded at this wavelength. To perform this assay, the Ferric Reducing Antioxidant Power reagent (FRAP) was prepared by mixing a buffer acetate solution at 300 mM (pH 3.6), with 10 mM of 2,4,6-tripiridyl-s-triazine (TPTZ) in 40 mM of HCl and $FeCl_3$ 20 mM. This mixture was then diluted in 1/3 of this volume with acetate buffer and allowed to stand in a laboratory oven at 37 ºC for 15 minutes. The samples were prepared in distilled water at 0.1 $mg.mL^{-1.}$. The control was made with FRAP reagent and distilled water, and the blank was made with distilled water and the sample. Each solution is prepared in quadruplicates and measured its absorbance at 515 using a plate reader (PowerWave XS, Bio-TEK) at 0 min and 4 min. The results were expressed as μM equivalents of Trolox, using a calibration curve made from Trolox.

3.5. Low molecular weight phenolic compounds quantification by HPLC-DAD

The low molecular weight phenolic compounds quantification was performed by High Performance Liquid Chromatography coupled with Diode Array Detector- (HPLC-DAD), by injecting 20 μL of the blackberry anthocyanic extract, which has been previously extracted by a liquid-liquid extraction. For this extraction, in a micro-tube, 600 μL of extract was added, along with ethyl acetate and acetonitrile, in a 1/2/2 ratio, respectively. The tube was mixed

and centrifuged during 5 min at 8000 rpm. The organic phase was removed into a new micro-tube, and the aqueous phase was extracted following the same process afro mentioned. The samples were then speed-dried in a speed Vaccum at 37ºC for 4 hours. Finally, the residue was resuspended in a mixture of MeOH and distilled water (1:1). The HPLC analysis was performed using a reverse phase column Merck C18 (LiChrospher® STAR, LiChroCART® 250-4, 150x4.6 mm d.i; 5 μm). The solvents used were H_2O/CH_3COOH (99:1, v:v) (Solvent A) and $H_2O/CH_3COOH/CH_3CN$ (79:1:20, v;v;v) (Solvent B). The flow used was fixed at 0.3 mL.min^{-1}. The results were expressed as μg GAE.mg^{-1} of extract, using a calibration curve of gallic acid. The elution gradient applied is presented in Table 5.

Table 5- Elution gradient used in the quantification of low molecular weight phenolic compounds.

Time (min)	A (%)	B (%)
0	80	20
55	20	80
70	10	90
90	0	100
90	80	20

3.6. Anthocyanins quantification and identification by HPLC-DAD and HPLC-DAD/ESI-MS

The quantification of anthocyanins present in the blackberry extract was performed by HPLC-DAD, injecting 20 μL of the extract (prepared at 1.0 mg-mL^{-1} in acidified water) in a reversed phase C18 column from Merck (LiChrospher® 100, LiChroCART® , 250x4 mm d.i; 5 μm) at 22ºC. Detection was performed between 200 nm and 700 nm. The mass detection was made by using a Finnigan LCQ DECA XP MAX mass detector, at a flow rate of 0.5 mL.min^{-1}, with an atmospheric pressure ionization and an electrospray ionization interface. In this detection, the capillary voltage was 4 V, with a capillary temperature of 325ºC. The mass spectra were obtained in the mode of positive ion, at an interval of *m/z* between 0 and 2000. Three scans were made: first, a full-mass; then, a zoom scan on the most intense ion; finally, a MS-MS of ion using relative collision energy of 30 V and 60 V.

The solvents used were H_2O/HCOOH (90:10) (A) and $H_2O/HCOOH/CH_3CN$ (60:10:30) (B) at a 1.0 ml.min^{-1} flow. Results were expressed as μg equivalents of Cy3glc.mg^{-1}, using a calibration curve made with cyanidin-3-*O*-glucoside. The elution gradient used is presented

in **Error! Not a valid bookmark self-reference.**. Anthocyanins identification was performed by HPLC-DAD/ESI-MS applying the same elution gradient at 0.5 ml.min^{-1} flow, with H_2O/HCOOH (99:1) (A) and H_2O/HCOOH/CH_3CN (69:1:30) (B).

Table 6- Elution gradient used in anthocyanins quantification.

Time (min)	A (%)	B (%)
0	80	20
70	15	85
75	0	100
85	0	100
90	80	20

4. Preparation of soluble/insoluble complexes derived from blackberry anthocyanins and λ-carrageenan

4.1. Solutions preparation

λ-CRG solutions were prepared in acetate buffer (10 mM) at different pH values (pH=2.5; 3.0 and 4.0). Briefly, λ-CRG (0.1 % w/w) solutions were prepared by dissolving the required solid amount in acetate buffer and heated in a pyrex tube at 80ºC for 10 minutes for proper dissolution. The solutions were allowed to reach room temperature (20 ºC) and the pH was adjusted, whenever necessary using either HCl 0.01 M or NaOH 0.01 M. Blackberry anthocyanic extract solutions (0.1 % w/w) were prepared in acetate buffer at room temperature. pH was adjusted, whenever necessary using either HCl 0.01 M or NaOH 0.01 M. Samples were equilibrated for at least 1h prior to their use and centrifuged at 13000 rpm for 2 minutes to remove any remaining insoluble impurities in the solution.

4.2. Coacervation conditions: determination of the optimal ratio

To determinate the optimal for coacervation conditions, preliminary turbidimetry assays were performed based on the method described in the literature (Tavares et al., 2021). These assays were performed in triplicate, in acetate buffer (10 mM) at three different pH values (pH=2.5; 3.0 and 4.0) at a total reagents concentration of 0.1% (w/w). Aliquots (5-100 μL) of λ-CRG solution at 0.1 % (w/w) were added stepwise to the anthocyanic solution at 0.1 % (w/w). The blank was made with distilled water. and the absorbance was measured

before the additions of λ-CRG. A small aliquot of λ-CRG was added to the UV-Vis cell and mixed for 15 seconds, using a parafilm to avoid spillage of the solution. The optical dispersion of these solutions was measured using an UV-Vis spectrophotometer (Evolution Array UV-Visible Spectrophotometer, Thermo Scientific) at 650 nm, in triplicates.

4.3. Zeta potential measurements

Zeta potential (ζ-potential) was obtained by ELS (electrophoretic light scattering), using a Malvern Zetasizer Nano ZS (Malvern Instruments Ltd, UK) machinery. To measure ζ, the dispersant used was water, the viscosity of the dispersant was 0.887 cP and its refraction index was 1.330. The dielectric constant measured was 78.5 F/m, the temperature was fixed at 25º C, and no equilibrium time was necessary.

To determinate the charge balance in the formation of insoluble complexes, all samples with phosphate/citrate buffer at 150 mM or acetate buffer at 10 mM, were filtrated before the reaction occurred. Samples were put in constant mixing for 2 hours. Then, they were centrifuged at 12500 rpm, at 20ºC for 10 minutes. 1 mL of the supernatant was placed in a cell appropriate for ζ-potential measurements. In the determination of the optimal pH to the formation of insoluble complexes, samples with acetate buffer at 10 mM, received the same treatment as the ones with phosphate/citrate buffer.

In the release study, ζ-potential was also determined. Samples of H_2O Millipore at pH=1.7, pH=5.4 or pH=7.4, PBS or MES were put in constant agitation for eight hours. Samples were centrifuged at 0h, 4h and 8h, at 20ºC, for 1 min at 12000 rpm. Then, aliquots of 1 mL of samples in pH=5.4, pH=7.4, MES and PBS were removed at 0h, 4h and 8h and its ζ-potential was measured. The samples at pH=1.7 were not measured due to limitations of the equipment. In all assays, three replicates were performed, and the data was presented as mean ± SD mV.

4.4. Preparation of insoluble complexes

Insoluble PECs between blackberry anthocyanins and λ-carrageenan (BbE-λ-CRG) were produced based on the polyelectrolyte complexation between anthocyanins positively charged and carrageenan's molecules negatively charged. A ratio of BbE/λ-CRG of 1:0.05, at a total concentration of 0.1 % (w/w) was used based on the turbidity experiments. The BbE was prepared at 0.1 % (w/w), in acetate buffer (10 mM at pH=3) and allowed to mix for 10 minutes and ultrasonified for 5 minutes. Then, the pH was adjusted using HCl 0.01 M / NaOH 0.01 M, when necessary. To produce insoluble complexes, 500 mL of BbE at 0.1 % (w/w) was put in a large beaker, and 25 mL of λ-CRG at 0.1 % (w/w) was added, and the

content was mixed for 2 hours at 120 rpm. The content of the flask was transferred to falcons and centrifuged for 10 min at 22 ºC at 12500 rpm, until the supernatant was clear. The pellets were washed two times, each with Millipore H_2O, to remove un-bound ANCs. After discarding the supernatant, the pellets were freeze-dried.

5. Physicochemical characterization of the anthocyanin-carrageenan complexes

5.1. Incorporation rate and loading capacity of λ-CRG

The amount of ANCs incorporated into the BbE-λ-CRG complexes at pH 3.0, was determined and expressed as the incorporation rate and loading capacity of λ-CRG. This determination was based on a method described in the literature (Klimaviciute et al., 2015). For this determination, the production of BbE-λ-CRG complexes were performed on small eppendorfs, in triplicates as previously described in Section 4.4. For control sample, the λ-CRG was replaced by acetate buffer at 10 mM at pH=3. The ANCs concentration of the supernatant was determined using the same method described in Section 3.6. The results were expressed as the incorporation rate and as g of Cy3glc *per* g of λ-CRG (loading capacity), using the following equations:

$$\text{Incorporation rate} = \left(\frac{(Cy3glc)_{control} - (Cy3glc)_{sample}}{(Cy3glc)_{control}}\right) \quad \text{Equation } (1)$$

$$\text{Loading capacity} = \left(\frac{(Cy3glc)_{control} - (Cy3glc)_{sample}}{(\lambda\text{-CRG})}\right) \quad \text{Equation } (2)$$

5.2. Scanning electron microscopy (SEM) and Cryo-SEM

The analysis of the morphology of the BbE, λ-CRG and BbE-λ-CRG insoluble complexes was performed by scanning electron microscopy (SEM), using a FEI Quanta 400 FEG ESEM/EDAX Genesis X4M equipment located in CEMUP (Materials Center at the University of Porto). The samples were secured in aluminum supports, and coated with a small Au-Pd layer, to increase electron conductivity, using a SPI Module Sputter Coater. The microscopic image of the surface of the insoluble complexes was obtained with an acceleration voltage of 15 kV, working distance of 10 mm and magnification level between 500x and 15000x.

BbE-λ-CRG insoluble complexes before freeze-drying were analyzed by Scanning electron cryomicroscopy (*cryo*-SEM). The analysis was carried out using a JEOL JSM 6301F Oxford

INCA Energy 350 electron microscope, equipped with a Gatan Alto 2500 cryo-preparation chamber. The insoluble complexes were vitrified in liquid nitrogen subcooled to -200 °C and fractured. Solvent sublimation took place at - 90 °C for 120 s and the sample was coated with an Au-Pd layer, using a SPI Module Sputter Coater. The obtention of the microscopic image was made at -150ºC, with an acceleration voltage of 15 kV, working distance of 15 mm and magnification level at 5000x.

5.3. Fourier Transform Infrared Spectroscopy with attenuated total reflectance (FTIR-ATR)

FTIR-ATR data of BbE-λ-CRG complexes, λ-CRG and BbE were obtained using a PerkinElmer Spectrum Two equipment (USA), at room temperature. To perform the analysis, approximately 1 mg of the sample were placed in an ATR crystal made from synthetic diamond. All spectra were obtained between 4000 cm^{-1} and 400 cm^{-1}. The experiments were carried at FCUP | DQB- Lab & Services, Porto, Portugal.

5.4. Thermal stability of blackberry extract- λ-carrageenan insoluble complexes

The thermal stability of BbE-λ-CRG complexes, was evaluated by simultaneous thermal analysis (STA), that combines dynamic scanning calorimetry (DSC) and thermogravimetry (TGA). BbE-λ-CRG complexes were analyzed, as well as the BbE and λ-CRG. The experiment was carried out at a heating rate of 5 ºC / min. To perform this assay, a STA7200RV from Hitachi Instruments, Inc. (Japan) was used. Solid samples with approximately 10 mg were placed in an open aluminum crucible. The assays were performed under inert atmosphere, and the measurement was made between 20 ºC and 400 ºC, at a heating rate of 5 ºC/min.

5.5. Anthocyanins release pattern from insoluble complexes

The behavior of insoluble complexes in five aqueous systems was studied. Insoluble complexes were prepared in 1.5 mL eppendorf's, at 5 $mg.mL^{-1}$ and dissolved in H_2O Millipore at pH=1.7, pH=5.4, pH=7.4,MES buffer at 10 mM (pH=5.2) or PBS buffer at 10 mM (pH=7.4), for 8 hours at 20ºC using an Advanced Vortex Mixer ZX3 from VELP Scientifica. MES and PBS were used to compare the release behavior with samples with only H_2O at three different pH, since salts concentrations and composition can change the release pattern. Aliquots of 200 μL were removed from the system at certain time intervals,

being replaced by the same amount of solvent. To determinate the amount of ANCs released, HPLC-DAD was used. This assay was performed in triplicates.

To understand the release pattern of BbE-λ-CRG nanocomplexes at different pH, the data obtained by HPLC, were fitted in Korsmeyer-Peppas mathematical model of drug release, using the following formula:

$M_t/M_\infty = Kt^n$ Equation (*3*)

In this equation, M_t , M_∞ , K, t and n refers to the amount of compound released in time t, the initial amount of compound in the sample, a constant that includes structural and geometrical properties of the compound, and release component, respectively (Sarkar et al., 2021). This equation can be simplified as:

$\log(M_t/M_\infty) = n\log(t) + \log(K)$ Equation (*4*)

According to the Korsmeyer-Peppas model, sing the equation above, the data can be plotted using a graph of log (M_t/M_∞) versus log t, up to the point where the percentage of release is above 60 %, *i.e.* until $M_t/M_\infty < 0.6$. Using this method, the slope of the curves was obtained via linear logarithmic equations and the coefficient of determination (R^2) was also calculated. The determination of ANCs in each time mark was performed by the same method described in Section 3.6.

6. Statistical analysis

Results were presented as form of mean ± standard deviation (SD) and was statistically treated using one-way ANOVA followed by the Tukey's test of multiple comparison to compare means between different columns. The data analysis was made using Prism 9.1.1 (GraphPad software).

Results and discussion

1. Characterization of the blackberry extract

The polyphenolic extract obtained from blackberries was characterized by UV-Vis spectrophotometry and HPLC-DAD evaluating its composition on phenolic compounds, monoglucosilated anthocyanins, protein, and antiradical and antioxidant activity. The obtained data is presented in Table 7.

Table 7- Physicochemical characterization and bioactive properties of blackberry extract. Data is presented as mean ± SD.GAE (gallic acid equivalents). TPC (total phenolic content). Low molecular weight phenolic compounds and anthocyanins were quantified by HPLC-DAD.

Composition of BbE	
Folin-Ciocalteau (TPC) (μg of GAE.mg^{-1} of extract)	390.0 ± 36.7
Low molecular weight phenolic compounds (μg eq. of GAE.mg^{-1} of extract)	72.9 ± 13.9
Anthocyanins (μg of Cy3glc.mg^{-1} of extract)	556.6 ± 65.1
Bradford (μg eq. of BSA. mg^{-1} of extract)	65.3 ± 11.4
Bioactivity of BbE	
DPPH (μM equivalents of Trolox)	19.7 ± 1.2
FRAP (μM equivalents of Trolox)	195.5 ± 17.8

The results obtained showed that the BbE extract was rich phenolic compounds (determined by the Folin-Ciocalteau assay) presenting a low content of protein, about 65.3 mg. g^{-1} of extract. ANCs, accounted for about 557 mg. g^{-1} of extract, while low molecular weight phenolic compounds corresponded to 73 mg. g^{-1} of extract. The chromatographic profile of low molecular weight phenolic compounds and anthocyanins, detected at 280 nm and 520 nm, respectively, in this extract is presented in Figure 10.

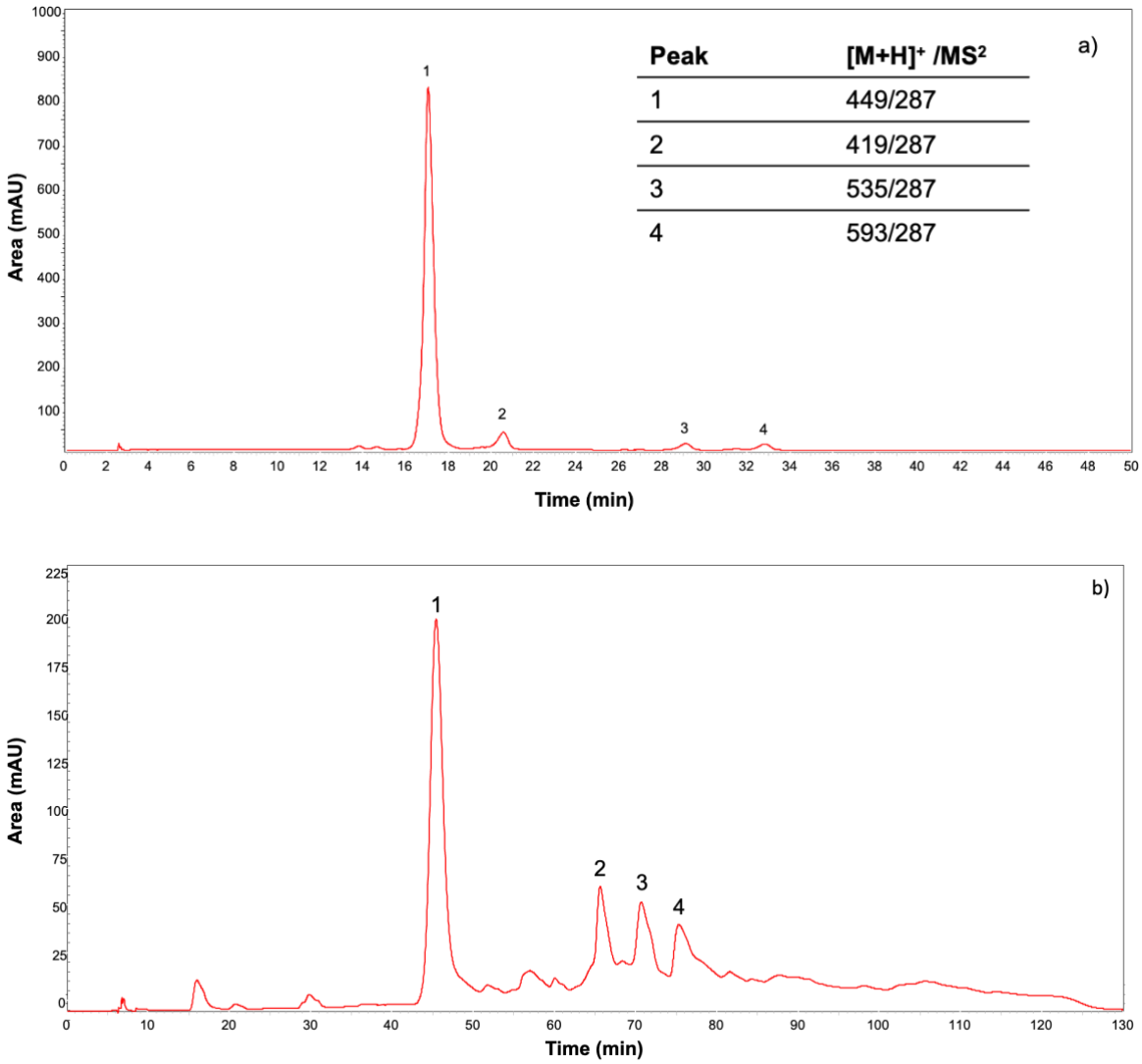

Figure 10- Chromatograms of the anthocyanins profile and low molecular weight phenolic acids, respectively, present in the blackberry extract.

The chromatogram corresponding to ANCs compounds in BbE showed four relevant peaks. cyanidin-3-*O*-glucoside (peak 1, Figure 10) was the most abundant ANC (90 %), followed by cyanidin-3-*O*-xylose (4 %), cyanidin-3-*O*-(6''-malonyl-glucoside) (2%) and cyanidin-3-*O*-dioxalyl-glucoside (2 %). Peak identification was performed based on HPLC-DAD/ESI-MS analysis and compared to previous literature reports on blackberry extracts (Fernandes et al., 2018; Marques et al., 2016).

A study of the antioxidant activity of garden blackberries that were extracted with MeOH, the TPC, by the Folin-Ciocalteu method, was 27.89 μg of GAE per mg of extract, in dry weight (Albert et al., 2022). Herein, the value recorded was 390 ± 36.7 μg of GAE per mg of extract, much higher than the value obtained in the literature. In the same study, the ANCs content that were obtained by HPLC-DAD, had a value of 7.733 ± 0.683 μg of Cy3glc

equivalents per mg of extract, being significantly lower that the characterization performed in the BbE.

The high content of ANCs may be reflected on the capacity of sequestering free radicals (19.7 ± 1.2 μM equivalents of Trolox) and reducing power (195.5 ± 17.8 μM equivalents of Trolox). In other studies, the capacity to eliminate free radicals, showed that a blackberry extracted with MeOH, had a higher percentage of reduction of antiradical activity(63.13 ± 3.45 %) , compared to 34.35 ± 3.99 % obtained herein (Albert et al., 2022).

Despite the comparisons made of the characterization of BbE, it is important to take into consideration that the blackberry extract does not have the same origin as the extract referred to in the literature, with respect to the soil type, temperature, humidity, and light during its planting. However, the results found in here showed that this BbE can add nutritional value due to its high composition of phenolic acids, ANCs and antioxidant and antiradical activity. Furthermore, the high content of ANCs of this extract can enhance the production of insoluble PECs.

2. Determination of the optimal conditions in the formation of BbE-λ-CRG complexes

The optimal conditions in the formation of BbE-λ-CRG complexes were obtained by turbidity measurements. The goal in this assay was to study the optimal weight ratio of BbE and λ-CRG, associated to the formation of aggregates (both soluble and insoluble) suspended in the liquid matrix. This study was performed at three pH's (pH 2.5, 3 and 4), using a UV-Vis spectrophotometer, measuring the absorbance at 650 nm, that can be referred as the optical dispersion (O.D). At slightly acidic pH, between pH 2 and 4, positively charged flavylium cation and the neutral hemiketal and quinoidal base coexist in solution. Given the previous studies concerning the interaction between ANCs and anionic polysaccharides, an electrostatic interaction is expected to take place, due to the interaction between opposite charges, namely, the flavylium cations of the ANCs and the negatively charged sulfate groups on CRG (Jeong & Na, 2012; Klimaviciute et al., 2015; Navikaite et al., 2016). Thus, the choice of the working pH range falls on the acid-base equilibria of these two compounds. At acidic pH, anthocyanins have positive charges due to the protonation of the C=O group (Cruz et al., 2015). On the other hand, in previous studies in the literature, the CRG presented negative charges across all pH's, due to the sulphate groups (Tapia et al., 2004). The optical dispersion was determined at various BbE/λ-CRG weight ratios, by the addition

of polysaccharide aliquots to the BbE extract solution at pH=2.5, 3 and 4. Results of the O.D are shown in Figure 11.

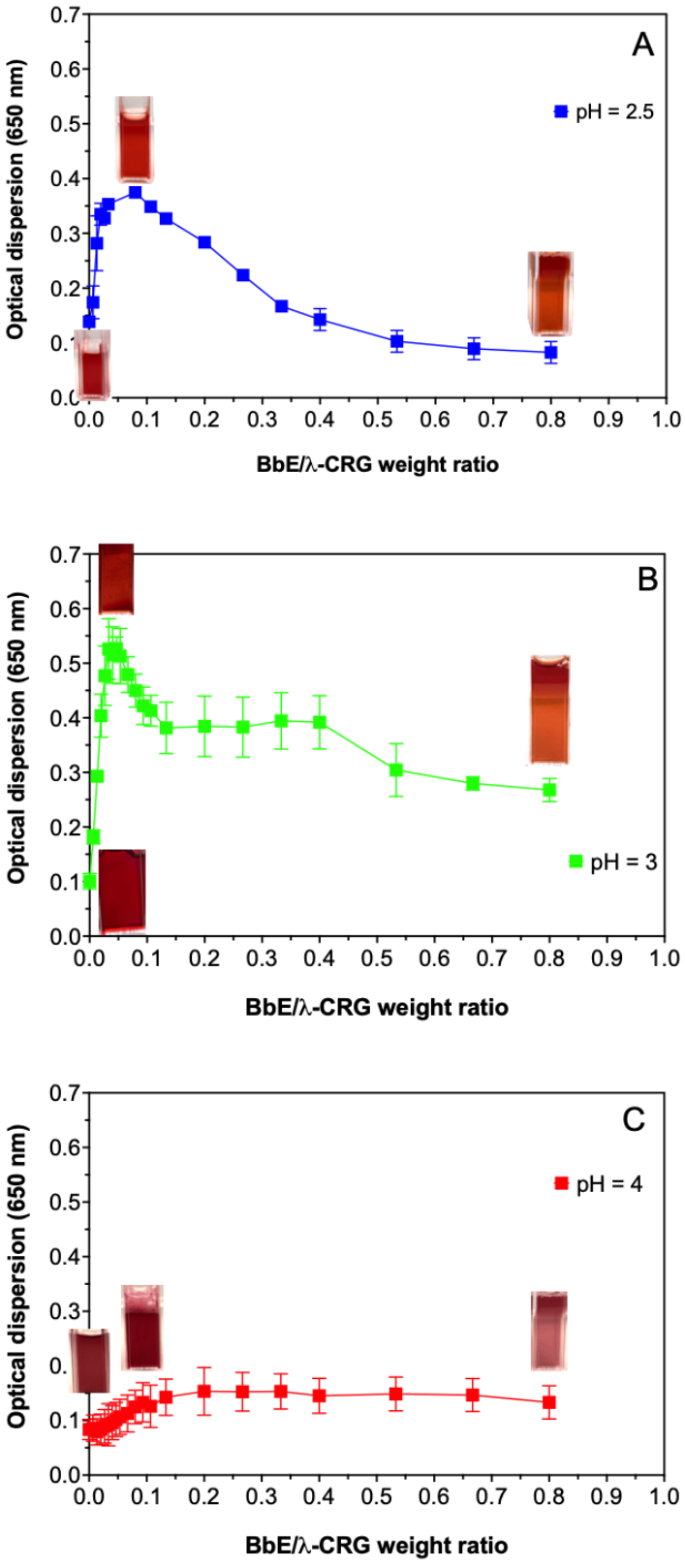

Figure 11- Optical dispersion of the blackberry complexation with λ-carrageenan at 650 nm at different weight ratios. A) pH = 2.5; B) pH = 3; C) pH = 4.

The application of turbidimetry was shown to be a suitable method for detecting the formation of molecular complexes. In addition, UV-Vis spectra are useful to prove complexation by non-covalent bonds, which are verified by absorbance and/or wavelength deviations (Eiro & Heinonen, 2002; Susanti et al., 2018).

During the titration experiments, the type of complexes formed (from soluble complexes to solid precipitates), was shown to be dependent both on the weight ratio of complex-forming reagents, pH and amounts of salts present in solution. From the results obtained, it could be observed that at pH= 2.5 (Figure 11-A), with increasing additions of λ-CRG, there was an increase in turbidity, related to the formation of insoluble complexes, until the maximum point of interaction (BbE/λ-CRG 1:0.08). From this weight ratio onwards the turbidity value began to decrease, reaching a constant value until BbE/λ-CRG=1:0.8. This sharp decrease should be related to the higher solubility of the complexes formed, that happens when the charge balance drifts away from the stochiometric charge ratio (Tavares et al., 2021). In fact, with the addition of more λ-CRG to the solution, some negatively charged sulfite groups remained free in solution, increasing the solubility of formed complexes (Dragan & Schwarz, 2004). It could also be observed that the color of the samples suffered a rapid alteration with the addition of λ-CRG, shifting from red (no λ-CRG was added) to orange at the point of maximum interaction, showing a hypsochromic shift. These changes in the absorbance spectra after λ-CRG addition indicated the formation of electrostatic complexes between the sulfite groups of CRG and anthocyanins cationic form. This color shift, as already been reported before in the literature for anthocyanins-anionic polysaccharides interaction, such as dextran sulfate or with other cation-exchange resins (Klimaviciute et al., 2015) .On the opposite, the formation of complexes between chondroitin sulfate and ANCs resulted on a bathochromic shift. In this work, besides the electrostatic interaction, provided by the sulfated groups in polysaccharides, hydrophobic and intermolecular stacking also played a significant role in complex formation, through N-acetyl groups (Jeong & Na, 2012). In the case of λ-CRG, its hydrophilic character due to the sulfite groups, which are ionized in acidic medium due not allow the hydrophobic interaction with anthocyanins.

At pH =3 (Figure 11-B), solution turbidity increased until BbE/λ-CRG weight ratio was close to 0.05. From this point on, solution turbidity began to decrease, reaching a plateau of similar values of turbidity, higher than those observed at pH 2.5. It was also possible to see changes in the color of the sample, from red to orange, possibly relate to the electrostatic interaction that occurs. The decrease of turbidity with the increase of the BbE/λ-CRG weight ratio, *i.e.*, increase of the addition of negative charges', is associated with the higher complex solubility. Finally, at pH = 4 (Figure 11-C), there was no significant increase in

turbidity at this pH, and the formation of large amounts of insoluble complexes was not noticeable. The red flavylium cation, AH^+ (Figure 5), is the predominant specie under sufficiently acidic conditions. When pH is raised, the flavylium cation is involved in two reversible and parallel reactions: deprotonation to give the quinoidal base (A) and hydration leading to the hemiketal (B) (Pina, 2014). At pH= 4, AH^+ is in fast equilibrium with A form thus, less flavylium cations are available to establish electrostatic interactions with λ-CRG. The color of the sample before the addition of λ-CRG was also an indicator that the acid-base equilibrium of the ANCs was being shifted to the formation of quinoidal forms.

A recent published study related to complex coacervation, was focused on the interaction between chitosan and whey protein isolate (Tavares et al., 2021). In this work, it was possible to observe that the turbidity increased along the ratios of chitosan/whey protein isolate, and was attributed to the coacervate formation, between chitosan and whey protein isolate. Besides that, it was possible to observe that the absorbance reached a constant region, associated to the saturation of chitosan molecules by the complexation of whey protein isolate, *i.e.*, the maximum turbidity before no insoluble complexes are formed (Tavares et al., 2021). Furthermore, the maximum interaction remained constant even with the addition of chitosan in large amounts, unlike what happened herein, where the O.D decreased upon the point of maximum interaction. Having the information on the measured O.D, the point of maximum interaction is related to a higher formation of insoluble complexes. These results were useful to optimize the production of insoluble complexes, giving information about the quantity of insoluble complexes that occur at three different pHs.

Furthermore, the pH chosen is determinant in the outcome of the complex's formation. Particularly, changes in the pH strongly influence the net charge of solid complexes and can result in a decrease of the stochiometric ratio of negative/positive charges, leading to conformational changes in the polymeric net of complexes. Having into account the information detailed, and to guarantee the maximum electrostatic interaction, the BbE/λ-CRG ratio used in the production of insoluble complexes was 1/0.05.

As previously described, pH can induce changes in the quantity and nature of the complexes formed (by changing the charge balance produced). Preliminary assays of turbidity were made to find the optimal anthocyanin-to-carrageenan mass ratio for the formation of insoluble complexes. The maximum optical dispersion was obtained in the BbE/λ-CRG mass ratio of 1/0.05 (w/w). Establishing the ratio chosen previously, the net charge formed during complexation reaction was also investigated at three different pHs, with acetate buffer. To perform this assay, stocks solutions of BbE (0.1%, w/w), λ-CRG

(0.1%, w/w) and the BbE-λ-CRG complexes at 1/0.05 weight ratio were prepared at pH= 2.5, pH=3 and pH=4, with acetate buffer at 10 mM. The solid precipitates of BbE-λ-CRG complexes were eliminated by centrifugation and the ζ-potential of the resultant supernatant, BbE and λ-CRG solutions was measured. These measurements are presented in Table 8.

Table 8- Values of ζ at three different pH's using acetate buffer, fixing the blackberry/λ-carrageenan at 1/0.05, expressed as mean ± SD; For each row, samples with the same symbol do not present statistical differences (p>0.05).

Samples	**ζ-potential (mV)**		
	pH=2.5	**pH=3**	**pH=4**
BbE	25.7 ± 0.6	12.5 ± 0.2	-15,1 ± 0,9
λ-CRG	-33.2 ± 0,5	-42.6* ± 1,9	-42.3* ± 0.8
BbE-λ-CRG	12.7 ± 0.5	-3.4 ± 0.4	-38.8 ± 0.9

Zeta potential measurements of BbE samples at different pH values, showed significant differences (p<0.05), with a ζ-potential decreased with the increase of the pH value, correlated to anthocyanins chemical equilibrium. Changes in the pH lead to the formation of new equilibrium forms that shifted ζ-potential to negative values, as observed at pH=4. Regarding the λ-CRG, the net charge was negative for all measured pH's, although this value where less negative at pH 2.5 (p<0.05). This result is in line with the values reported in the literature, showing negative charges even at acidic pH (Tapia et al., 2004). For BbE-λ-CRG complexes, significant differences could be observed in the ζ–potential value (p<0.05). AtpH=2.5 it was recorded a positive value of ζ-potential, becoming negative at pH=3 and pH=4. It is important to notice that when ζ-potential is close to zero, as in the case of pH 3.0, a quicker phase separation, *i.e.* the precipitation of insoluble complexes from the liquid phase occur (Espinosa-Andrews et al., 2013). This behavior is consistent with the fact that charge neutralization between charged moieties was achieved. If the value of ζ-potential drifts away from 0, electrostatic interaction in the complex may become weaker, thus affecting the physical properties of the complexes (Espinosa-Andrews et al., 2013). Complex coacervates made by the interaction of gum Arabic and chitosan were studied regarding their viscoelastic properties obtained by changing the ratio of the two biopolymers (Espinosa-Andrews et al., 2013). The results obtained showed that as the ratio of gum Arabic-chitosan was deviated from a specific range (3:1 to 5.5:1 meaning gum

Arabic-chitosan), ζ-potential deviated from the stoichiometric ratio, the yield of coacervates decreased, thus leading to an increased on the production of soluble complexes. (Espinosa-Andrews et al., 2013). According to our results, with the increase of BbE/λ-CRG ratios, the turbidity values decreased, resulting on lower amount of insoluble complexes, possibly due to weaker electrostatic interactions Additionally, at pH 3.0, the formation of insoluble complexes was higher, compared to the other pH's tested, in accordance the close to zero ζ-potential value. Therefore, the results obtained are in line with those that were obtainable by turbidity, as the maximum O.D achieved was also at pH=3.. Given the obtained results, the interaction at pH=3 at a 1/0.05 weight ratio (BbE/λ-CRG) were established as the optimal conditions for the formation of insoluble complexes.

In order to study the impact of salts in the coacervation reaction, this complexation was performed in citrate-phosphate buffer at 150 mM. In addition, the phosphate-citrate buffer could be used over a wider range of pHs. (Timilsena et al., 2019).

Thus, complexes formation was studied at five different pH values (2.5; 3; 3.5 ;4 and 5) using phosphate-citrate buffer at 150 mM, at a fixing weight ratio of 1:0.05 (w/w) After sample centrifugation, the ζ-potential value of the supernatants was measured (Table 9).

Table 9-Values of ζ-potential at five different pH's using citrate-phosphate buffer at 150 mM, expressed as mean ± SD. For each row, samples with the same symbol (*,**) do not present statistical differences (p>0.05).

Samples	**ζ-potential (mV)**				
	pH=2.5	**pH=3**	**pH=3,5**	**pH=4**	**pH=5**
BbE	18.9 ± 1,8	12.6 ± 2.0	-3.5 ± 0.8	-5.8 ± 2.5	-15.6 ± 3.4
λ-CRG	-45.5 ± 2.9	-49.8 ± 3.2*	-38.2 ± 2.3	-51.0 ± 2.6*	-48.9 ± 4.4*
BbE-λ-CRG	-8.0 ± 2.8	-23.4 ± 4.4	-41.5 ± 2.5*	-42.2 ± 2.5*,**	-45.0 ± 3.8*,**

At pH=2.5, the ζ-potential recorded in the BbE was 18.9 ± 1.8 mV, being the highest value of the five pHs. Statistical analysis showed that at pH 3.5 and 4.0, there were no statical differences (p>0.05). The positive/negative value of ζ-potential in BbE can be explained by the acid/base equilibrium in small increases in pH's. The increase of pH can lead to the formation of charged negative structures (quinoidal bases). This equilibrium is responsible to the negative values recorded at pH=4 and pH=5. On the other hand, λ-CRG, had a similar

negative ζ-potential values in the tested pH range, being slightly less negative at pH 3.5. The negative value of ζ is due to CRG structure with three sulfate groups that may ionized, bearing a negative charged. In fact, the pKa of λ-CRG is below 2, therefore, when pH > *p*Ka, this translates into a higher quantity of negative charge, which can explain the fact that the values of pH had no significant differences (Karimi et al., 2018).

The ζ-potential value of the complexes was shown to be negative at all measured pH's, which may be caused by the charge balance between each of the individual components, being also more negative as the pH increased. The negative ζ-potential value in these samples may also be justified by the ionic strength of the phosphate-citrate buffer, which is higher than the acetate buffer, having a direct effect on the measurement of ζ-potential value(Bhattacharjee, 2016). The statistical analysis showed that were no significant differences between pH=4 and pH=5, meaning that this increase of pH, did not have significant effect in net charge. Between pH=2.5, pH=3 and pH=3.5, significant differences could be observed. The formation of insoluble complexes is highly dependent on the pH and ionic strength, factors that were tested when finding the optimal conditions of this reaction. The use of phosphate-citrate buffer, a buffer with higher ionic strength than the acetate buffer, had negative impact on the course of the coacervation reaction. When the pH and buffer was changed, the charge stoichiometry of the mixture was being shifted from its maximum, leading to an excess of negative charges, consequently, less formation of insoluble complexes. The addition of salt can negatively impact the electrostatic interaction between two oppositely charged molecules, making them weaker (Blocher McTigue & Perry, 2020).

In conclusion, it was possible to verify that changes in the pH had direct impact on the formation of insoluble complexes. Furthermore, the increase of the ionic strength and the composition of the buffer used to produce these complexes, had negative impact on the reaction, weaking the electrostatic interactions between ANCs and λ-CRG. The use of acetate buffer at 10 mM and at pH=3 (and a mass ratio of 1:0.05) was the most adequate solvent to produce insoluble complexes, being possible to distinguish the coacervate rich phase (insoluble complexes) and the dilute phase.

3. Production of BbE-λ-CRG insoluble complexes

The production of insoluble complexes was performed at pH=3 at an BbE/λ-CRG weight ratio of 1/0.05. The profile of ANCs in BbE extract before and after complexation was performed, at BbE- λ-CRG complexes, with a ratio of 1/0.05, to determine the incorporation

rate and the g *per* g of CRG. The residual concentration of anthocyanins was determined in the supernatant, after centrifugation. Chromatograms are displayed in Figure 12.

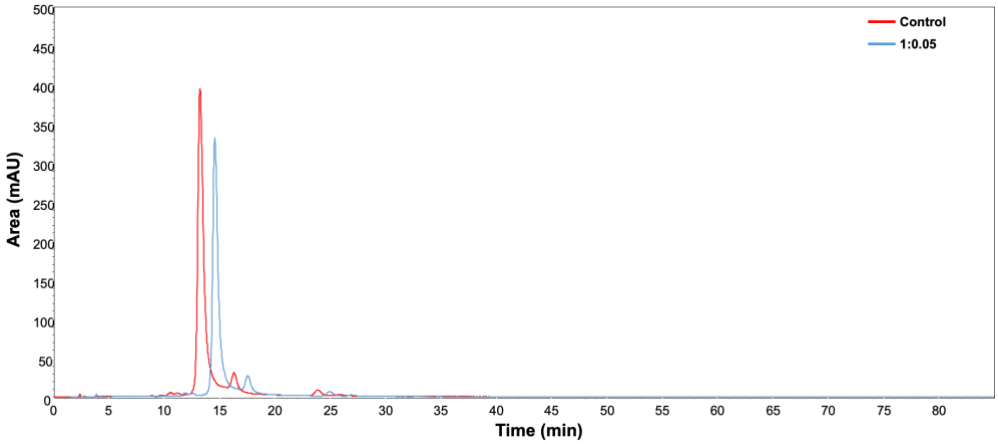

Figure 12- HPLC-DAD chromatogram. The red line, the control sample of the reaction of coacervation (the λ-CRG was replaced by acetate buffer). The blue line, the chromatogram profile after the addition of - λ-CRG, at a ratio of 1/0.05.

Chromatographic analysis of the supernatant of the control and ANT-λ-GRG complexes at the ratio of 1/0.05 (BbE/λ-CRG) provided information on the incorporation rate of ANCs and loading capacity of λ-CRG. Besides that, Cy3glc, the most abundant ANC presented the most significant changes after complexation. The incorporation rate of ANCs obtained was 12.26 ± 1.68 %, which reflected on the chromatographic profile in Figure 12, where it is possible to observe a decrease of the area of the first peak, comparing to the control sample. This value is associated to the percentage of insoluble complexes that are formed during the reaction of coacervation, as the formed soluble complexes can be destroyed in the acidified solution to determine anthocyanins concentration. The loading capacity was 1.11 ± 0.15 g of Cy3glc *per* g of λ-CRG. In a similar study, the incorporation rate of ANCs from *Vaccinium myrtillus* in κ- and ι-CRG was determined, (Navikaite et al., 2016). At a weight ratio was 0.4/1 (CRG/ANC), at a total concentration lower than 0.07 g. L^{-1}, the incorporation rate was around 1.5 g of ANCs per g of ι-CRG (Navikaite et al., 2016). Furthermore, it was found that there were variations on the value of incorporation rate, with the increase or decrease of the total reagent concentration and weight ratio. The difference between the value determined herein and the one reported previously could be attributed to this variation. Using a different polysaccharide, the complexation of ANCs from *Vaccinium myrtillus* with dextran sulfate was investigated in the literature (Klimaviciute et al., 2015). Dextran sulfate is a polysaccharide widely applied in the pharmaceutical industry, that have three sulfate groups in its molecular structure, which can be responsible to form electrostatic interactions with ANCs (Klimaviciute et al., 2015). The results showed that

when the ratio of dextran sulfate/ANCs was 0.4, at a total concentration of 0.66 g. L^{-1}, the incorporation rate of ANCs was 73.7%, while the loading capacity of dextran sulfate was 1.7 g of ANCs per g of this polysaccharide. Additionally, using a different approach of stabilization, some authors studied the incorporation of ANCs from *Carissa carandas* in a biopolymer-based coacervate, with chitosan and pectin. The incorporation rate reported was 47.77%.

4. Physicochemical characterization of BbE-λ-CRG insoluble complexes

Freeze-drying of the insoluble complexes of BbE-λ-CRG resulted in a red-dark particulate material, as seen in Figure 13.

Figure 13- Prepared insoluble complexes of BbE and λ-CRG.

4.1. Morphology analysis of insoluble complexes

The morphological structure of freeze-dried BbE, λ-CRG, BbE-λ-CRG insoluble complexes was characterized through SEM analysis. The obtained microscopic images of the three samples are shown in Figure 14.

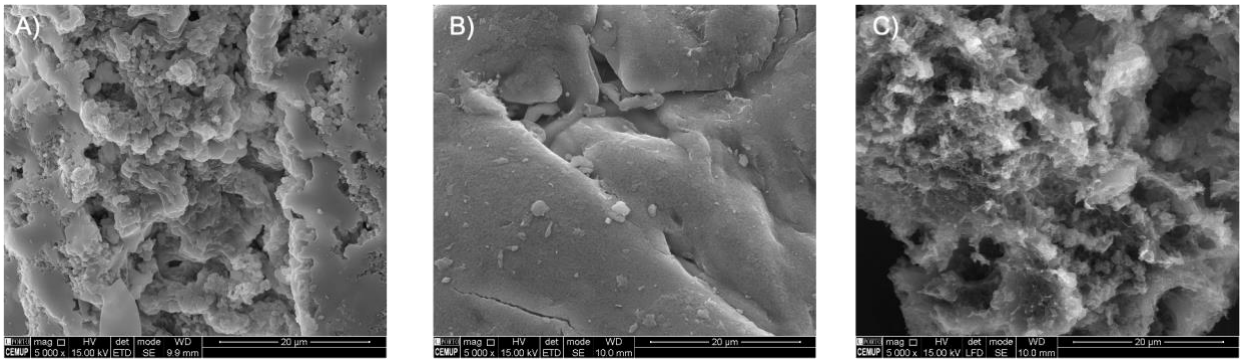

Figure 14 - Microscopic images obtained by SEM. A) blackberry extract powder; B) λ-carrageenan; C) blackberry-λ-carrageenan after freeze-drying.

From Figure 14, it could be observed that the BbE presented a compact structure, with a wrinkled surface. On the other hand, the morphology of the λ-CRG showed a much smoother surface with some filamentous and irregular shapes. The BbE-λ-CRG insoluble complexes after the freeze-drying process, presented a homogeneous structure, with several porous on the surface and with a reticular net shape. The microscopic image of these complexes suggests that the complexation took place, since it led to a different network structure, possibly due to the establishment of electrostatic interactions between anthocyanins and carrageenan, providing the formation of insoluble complexes with three-dimensional structure (de Souza et al., 2009). This disorganized structure is characteristic in coacervates, as reported in the literature (Meka et al., 2017). The *cryo*-SEM technique allows the morphological characterization of insoluble complexes structure in their native environment before the freeze-drying process, where substantial structural changes may occur (de Souza et al., 2009). Thus, *cryo*-SEM analysis was also performed to better characterize the morphological structure of the wet insoluble complexes. The results obtained from Cryo-SEM are shown in Figure 15 at different magnifications. The insoluble complexes showed a compact structure, with a continuous network and tight net mesh, with several porous and hollows. This morphological characteristics are usually observed in hydrogels (Polat et al., 2020).

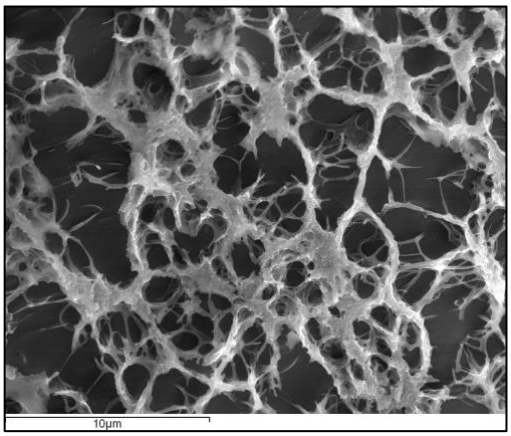

Figure 15- Low-temperature scanning electron microscopy (*cryo*-SEM) image of blackberry-λ-carrageenan coacervates at a weight ratio of 1:0.05 (w/w). Magnifications of 5000x. The accelerating voltage was 15 kV and working distance 15 mm.

In a recent study, morphological studies of formed coacervates from pectin and chitosan, for the encapsulation of ANCS, showed that coacervates loaded with ANCs did not display micropores, contrary to the coacervates without loaded ANCs (Sarkar et al., 2021). This absence of micropores after the encapsulation was attributed to the encapsulation within the free sites present in the blank coacervate. Soybean protein isolate and chitosan coacervates were also evaluated in terms of its morphological properties (Huang et al., 2012). The authors suggested that the interaction formed by PECs complexes, resulted in the formation of porous-like network structure.

4.2. Fourier Transform Infrared Spectroscopy FTIR-ATR

Fourier Transform Infrared Spectroscopy with attenuated total reflection (FTIR-ATR) was performed to evaluate the differences in the functional groups of the produced insoluble complexes and to investigate possible interactions between the reagents forming materials. The FTIR-ATR spectra of BbE, λ-CRG and BbE-λ-CRG insoluble complexes are shown in Figure 16.

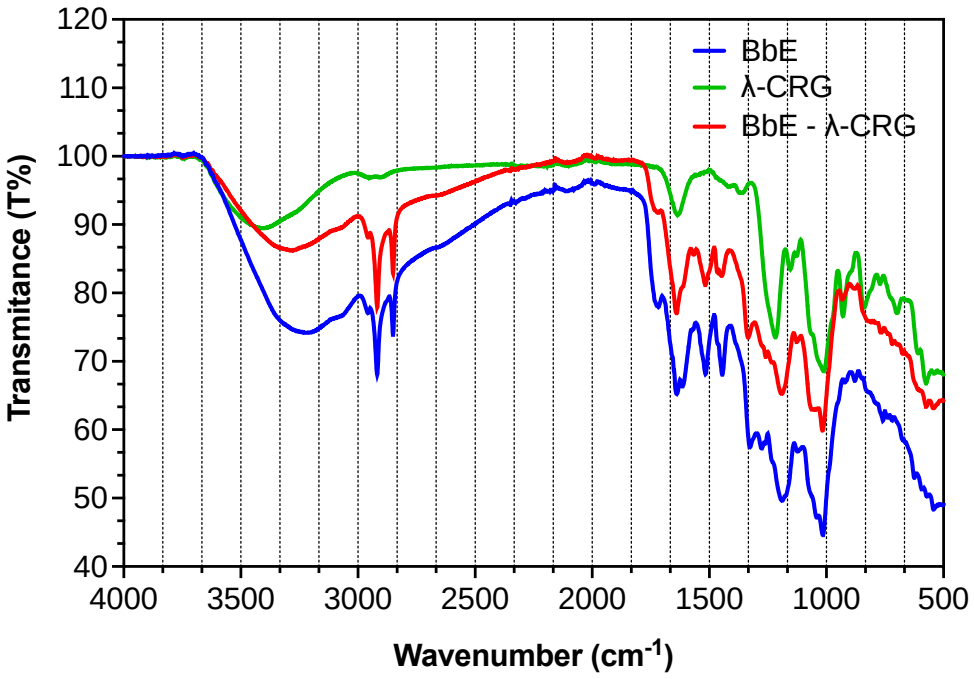

Figure 16- FTIR-ATR spectra of blackberry extract (blue color), λ-carrageenan (green) and the blackberry extract- λ-carrageenan complexes (red).

From the FTIR-ATR spectra of BbE, it was possible to identify several relevant groups. ANCs from the BbE showed a broad O-H stretch band at 3234 cm^{-1}, associated with the vibration of -OH bonds. A strong band was noticed at 1685 cm^{-1}, which was attributed to the stretching vibration of C=O in the benzopyran ring. At 2915 cm^{-1}, a stretching vibration of C-H bond was identified. Regarding the λ-CRG, the FTIR-ATR spectrum also showed a broad O-H stretch band, at 3400 cm^{-1}, again attributed to -OH groups. The sulfite group (SO_3^-) was also identified at 1220 cm^{-1}. For the insoluble complex, the characteristics FTIR bands of anthocyanic extract are dominant in combination with the spectra of λ-CRG, possibly due to the higher weight ratio of the pigment, related to the biopolymer.

The stretching vibration of the O-H bond was identified at 3251 cm^{-1}, with a higher wavenumber than the BbE, possibly due to the interaction of ANCs and λ-CRG, thus suggesting the occurrence of hydrogen bonding. The stretching vibration of the C=O bond in the benzopyran ring was also identified in the complexes of BbE-λ-CRG, however, at a higher wavenumber and lower intensity, which can be caused by the interaction with λ-CRG molecules. Finally, the sulfite group was identified at 1183 cm^{-1} with lower intensity. The deviation of the wavenumber and the lower intensity could be indicative that the complexation took place, probably due to the occurrence of electrostatic interaction between the positive anthocyanin flavylium cation and the negatively charged sulfite groups of CRG. In a similar study, where complexation of ANCs from *Vaccinium myrtillus* with CRG

was studied, it was observed this type of behavior (Navikaite et al., 2016). Additionally, all bonds identified are in Table A1. The interaction of ANCs and λ-CRG, may be caused by negatively charged sulfite groups and the positive charge in the benzopyran ring of ANCs. Variations in terms of its wavenumber of intensity, of these two bonds showed that the complexation was successful.

4.3. Thermal stability analysis of BbE-λ-CRG insoluble complexes

The thermal properties of food ingredients are extremely important for its industrial applications, as thermal processing is a common procedure during food processing. Thermal analysis of BbE, λ-CRG and BbE-λ-CRG complexes was evaluated by thermogravimetry (TGA), in terms of weight loss with the increase of temperature, and derivate thermogravimetry (DTG), that results on the derivation of the TGA curve. The obtained TGA and DTG curves is presented in Figure 17.

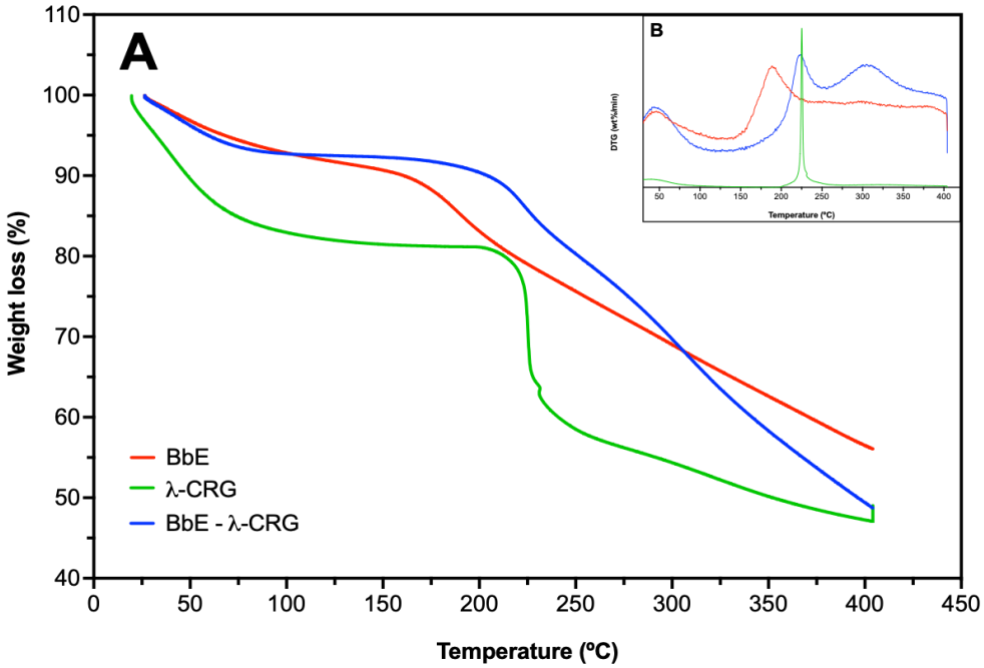

Figure 17- Data obtained of the thermal stability. A) Thermograms of all samples; B) DTG data.

Accordingly, to the TGA data in Figure 17A, the BbE showed a fast degradation along the increase of temperature, having a total of 43,86 % of mass loss. It is possible to distinguish two phases of degradation: the first, at nearly 50 ºC, is related to water loss (6,57 % of weight loss); the second phase, at nearly 193 ºC, is related to ANCs degradation (36,83 % of weight loss). From the DTG data, the temperature where the maximum degradation occurs (T_{peak}) was recorded at 194ºC. A study performed on the thermal degradation of Cy3glc extracted from blackberries, also showed two phases of degradation at similar

temperatures (Souza et al., 2020). The λ-CRG showed two stages of degradation, having a total weight loss of 52.87%. The first phase was detected at around 50 ºC, corresponding to 10,91% of weight loss. This can be related to water loss trapped in the λ-CRG powder, since it is a biopolymer with a tendency to absorb moisture, as seen in the literature, where TGA was performed in ι-CRG, where the results were similar (Jumaah et al., 2015). At 230 ºC it is possible to observe the second stage of degradation, that resulted in 35.89% of weight loss, and was possibly related to sulfite groups leaving the main structure and degradation of the carbohydrate backbone (Jumaah et al., 2015). The minimum temperature before thermal degradation (T_{onset}) was observed at roughly 200 ºC and the T_{peak} was observed at 225ºC. The insoluble complexes of BbE-λ-CRG showed two phases of degradation at similar temperatures and weight loss values, compared to the thermogram of BbE. A first stage of degradation was seen at 50ºC, resulting in 7.05% of weight loss and was attributed to water loss. The second stage of degradation was seen at 225ºC, and it can be related to the remotion of sulfite groups of the λ-CRG molecule. Data shown that the T_{onset} remained the same as the BbE profile (160ºC), however, the T_{peak} was shifted to higher temperatures, at 225ºC.

The TGA profile of the BbE-λ-CRG was similar to the one obtained on the BbE, however, the plateau of rapid degradation seen before, was achieved at higher temperatures. Additionally, the T_{peak} was observed at higher temperatures (31ºC higher), compared to the BbE, which may indicate that the complexation improved the thermal stability of BbE. In a previous work, zedo gum and gelatin were used, to encapsulate ANCs (Gharanjig et al., 2020). The results of the thermal stability showed that the formed coacervates had a better thermal stability than the free zedo gum. This was associated with the stronger interaction between gelatin and zedo gum (Gharanjig et al., 2020). In this case, the improved thermal stability may be associated to the incorporation of λ-CRG. Unlike the TGA thermograms, the DTG curves can clearly show the thermal decomposition of each individual sample. While the BbE and λ-CRG had one peak, the formed insoluble complexes had two peaks, suggesting that the electrostatic interaction was beneficial to the improvement of the thermal stability. These peaks were in the same area of the BbE and λ-CRG, however, they were shifted to higher temperatures, proving the enhanced thermal stability. Furthermore, the second peak from the DTG of the BbE-λ-CRG complexes can be related to a temperature shift by the same peak observed in the λ-CRG.

The DSC technique is used for analytical confirmation of the formation of samples that are in solid form. It can give information about the physicochemical properties of a material, as a function of temperature. The obtained DSC data is shown in Figure 18.

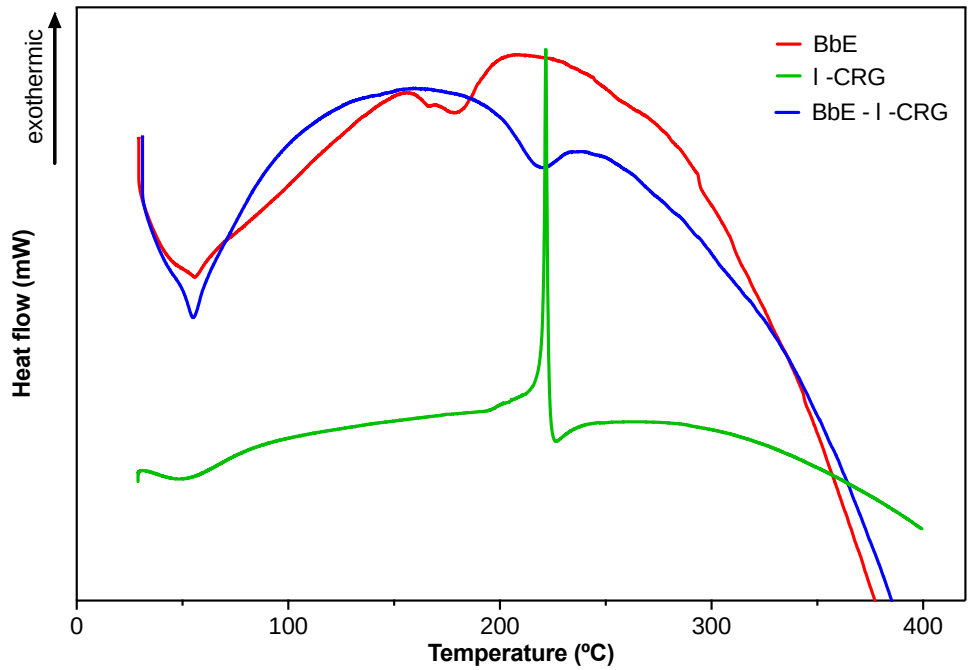

Figure 18- DSC curves from the BbE, λ-CRG and BbE-λ-CRG complexes.

From the data obtained by DSC, BbE (Figure 18), had two endothermic peaks, one from 50ºC until 100ºC, and from 163ºC to 202ºC. The λ-CRG had a strong exothermic peak from 206ºC until 233ºC, which may be related to the melting point of this polysaccharide. The BbE-λ-CRG complexes showed two endothermic peaks, the first at the same temperature of the peak recorded in the BbE. On the other hand, the second endothermic peak was recorded at the same temperature area as the one seen in λ-CRG, which may suggest that this peak is related to the transition phase verified in the λ-CRG sample. The second endothermic peak recorded in the BbE is not contained in the chromatogram of the mixture, i.e. it may indicate that there has been an enhancement of the thermal stability of the ANCs present in the extract, and successful complexation. In the literature, the thermal stability of blackberry ANCs encapsulated in b-cyclodextrin was studied (Fernandes et al., 2018). The results of the DSC assay showed that the encapsulation improved the thermal stability, since the same endothermic peak in BbE was shifted to higher temperatures, a similar behavior as the one observed for the produced insoluble complexes.

4.4. Release pattern: desorption study

The incorporation of ANCs in λ-CRG can improve the stability of these flavonoids, however, it is important to study the release of the main component at different pH values. To achieve this, the desorption study was performed in five media: H_2O at pH=1.7, 5.4 and 7.4; MES

at 10 mM (pH=5.2), and PBS at 10 mM (pH=7.4). The experimental data, in the form of the cumulative release rate is presented in Figure 19.

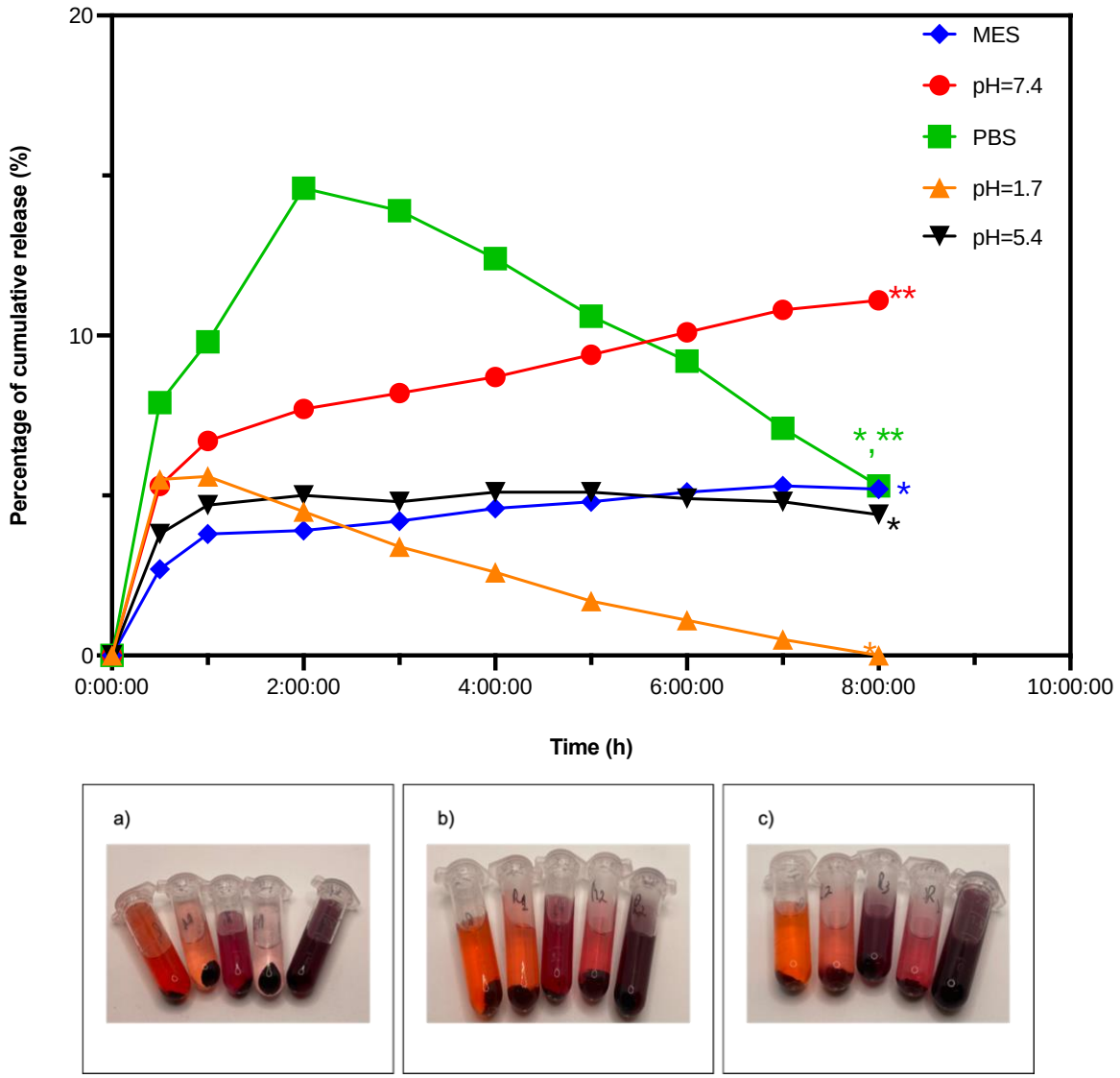

Figure 19- On top, ANCs release rate in five different solvents. At the 8-hour mark, samples with the same symbol (* or **) are not statistically different (p>0.05). On the bottom, color of the samples in the ANCs release pattern study. From left to right in all pictures: pH=1.7, pH=5.4, pH=7.4, MES, and PBS. a) t= 0h; b) t= 4h; c) t=8h.

At the 0-hour mark, there was a release of ANCs from insoluble complexes, with this release being more noticeable in PBS (16.5 ± 2.4 %), followed by pH=1.7 (5.6 ± 0.4 %), pH=5.4 (2.6 ± 0.3 %), pH=7.4 (2.4 ± 0.1 %) in water. The lowest initial concentration was obtained in MES (1.8 ± 0.1 %). This early release is in accordance with the color of the respective samples at the 0-hour mark (Figure 19).

The results of the cumulative release at each hour, showed that at pH=5.4 (H_2O) and MES, the release of ANCs reached a plateau after 1 hour of study. The intensity of the color

observed in the beginning of the assay did not change drastically. In pH=7.4, the release of ANCs was drastic until 1 hour of study, increasing it until the end of the assay. On the other hand, PBS and pH=1.7 release samples, showed a decrease of the ANCs release after the 2-hour mark and 0.5-hour mark, respectively. This decrease on the quantity of released ANCs, seemed to indicate that the effect of the dilution of original sample, when small aliquots were removed, was higher than the diffusion of ANCs from the insoluble complexes.

At pH=5.4, there was no significant impact of the insertion of a different salt composition on the dissolution of ANCs. On the other hand, the low release of ANCs may be because MES free acid does not have the capability to form coordination complexes with λ-CRG molecules. At pH=5.4, it seems that the release of ANCs achieves an equilibrium, between the contribution of the rate of diffusion of ANCs, and the dilution factor.

In the literature, the release pattern of ANCs in the coacervation between chitosan and pectin, for improving bioaccessibility of ANCs was also studied (Sarkar et al., 2021). The results showed that ANCs were released in a higher degree at pH=1.7, while in this work it was shown that at this pH, the quantity of ANCs became lower as time passed. Furthermore, at pH=7.0, it was obtained the lowest percentage of ANCs release (around 40%) (Sarkar et al., 2021). According to the same article, the degree of release was directly attributed to the swelling of the coacervate formulation, which was demonstrated to be high at lower pHs (Sarkar et al., 2021). The swelling had a direct impact on the release of ANCs from the electrostatic bond, therefore, the data obtained was plotted to a release pattern model that could consider this factor. To do this, the data was plotted in the Korsmeyer-Peppas equation. This model was originally developed to study how pharmaceutical drugs could be released from a polymeric system, which is adequate to the type of study in this work (Korsmeyer et al., 1983). This model considers the diffusion of water into the polymeric system, dissolution of the drug (in this model, ANCs) and swelling of the polymeric chain (Singhvi & Singh, 2011). Furthermore, this model only considers the first 60% of the release ($M_\infty < 0.60$). The plotted data showed a good coefficient of determination ($R^2 > 0.98$) throughout all samples. PBS and pH=1.7 ANCs release data were not considered due to the limitations of the Korsmeyer-Peppas model. The data is represented in Figure 20.

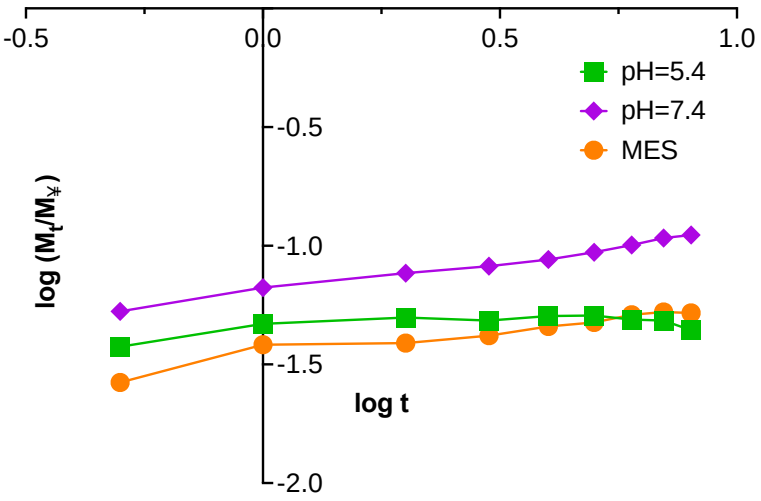

Figure 20- Korsmeyer-Peppas plot of data obtained by release rate in different medium.

The plot of the data from the release study is used to determinate the value of k and n, two coefficients that gives information on how the release occurs, under the diffusion law of Fick. The law of Fick describes the time of a transfer of solutes when a gradient of concentration is obtained (Siepmann & Siepmann, 2012). In this case, the release can be dominated by phenomena of diffusion and rearrangement of polymeric chains in the produced insoluble complexes. The release of ANCs by diffusion happens when water enters the surface of the polymeric system, it swells, and the ANC is dissolved and leaves the complex structure by diffusion (Colombo, 1993). The swelling rate at which ANCs leaves the polymeric system, determines how the release behaves (Khan et al., 2022). For this, following the Korsmeyer-Peppas model, the determination of n defines the type of transport. When n=0.5, the release follows the Fick's law, mainly caused by diffusion. On the other hand, if n=1, the transport of solutes does not follow Fick's law and the release follows the zero law of kinetics. Finally, if n is between 0.5 and 1, the release is considered an anomalous transport, mainly caused by diffusion, and swelling, which indicate that the release is mainly dependent on time. The dependence on time indicates that when n is located between those values, the release follows a first order kinetics. At pH=5.4 the value of n recorded was 0.05, at pH=7.4 n=0.26 and in MES n=0.21. All these values are above the threshold of $n < 0.43$, which indicates that in these medium, the release follows a Fickian diffusion mechanism (Supramaniam et al., 2018). This means that when the water enters the polymeric matrix, the rate of anthocyanins' diffusion is higher than the rate of polymeric relaxation.

Additionally, ζ-potential value was measured at 0h, 4h, and 8h, of the supernatant in each medium, aiming to understand the variation of the net charge presented in each model.

Data from the pH=1.7 samples were not presented due to limitation on the ζ-potential measurements, that cannot be made at acidic pH. The obtained results are presented in Table 10.

Table 10- ζ-potential expressed as mean ± standard deviation; Same superscripts (a-f) means there is not a significant difference between the values in the same column.

Time (h)	**ζ-potential (mV)**			
	MES (10 mM)	**H_2O pH = 5.4**	**PBS (10 mM)**	**H_2O pH = 7.4**
0	-26.8 ± 7.2	-24.2 ± 1.6	-30.7^{A} ± 1.0	-54,4± 0.9
4	-47.4^{A} ± 2,3	-33.9 ± 0.8	-30.9^{A} ± 1.3	-57,8 ± 0.9
8	-49.4^{A} ± 0,8	-46.2 ± 1.2	-36.2 ± 1.9	-62,7 ± 0.5

The release pattern of ANCs in MES was followed by a decrease of the ζ-potential , having a drastic variation from the 0-hour mark until the 4-hour mark. This was observed in the release pattern since the release of ANCs was higher from the 0-hour mark until the 1-hour mark. On the other hand, there was a slight increase of the ζ-potential from 4h to 8h, suggesting a low increase of the release of ANCs. According to the results in Figure 19, the release maintained a plateau until the 8-hour mark, which may explain why ζ-potential did not increase. When using water at pH=5.4, there was a drastic decrease of the measured ζ-potential after the 4-hour mark, which did not result in a higher release of ANCs. Drastic changes of ζ-potential were not observed in PBS, which was translated in a decrease of the release of ANCs at each hour. At pH=7.4, the measured ζ-potential was more negative as time elapsed, which was in accordance with the pattern release of ANCs observed at this pH.

Conclusion and future perspectives

ANCs are polyphenolic pigments that have a high potential both as a food additive, in the form of a colorant, and as a nutraceutical with beneficial health properties for humans when consumed. However, these pigments present a high instability in their free form, and, for this reason, it was hypothesized in this work their protection through the formation of ANCs and λ-CRG polyelectrolyte complexes Extract characterization showed that it has a high amount of monoglucoside ANCs. The anthocyanic profile of this extract showed that the most abundant ANC was Cy3glc. This extract has shown antiradical and antioxidant activity. During the formation of PECs, it was possible to observe that the ideal weight ratio for the formation of insoluble complexes would be 1/0.05, using acetate buffer at pH=3.

The morphology of the insoluble complexes revealed that they had an irregular and porous shape, with a compact structure. BbE-λ-CRG complexes in water demonstrated a morphology like a hydrogel.

The ANCs profile of BbE-λ-CRG complexes, demonstrated that Cy3glc is the ANC responsible for the electrostatic interaction with λ-CRG molecules, due to the decrease upon the complexation. Furthermore, ANCs from the BbE had an incorporation rate of 12.26 ± 1.68 %, which gave information on the quantity of insoluble complexes that were formed. 1.11 ± 0.15 g of Cy3glc equivalents were complexed per g of λ-CRG.

The thermal stability study showed that the complexation of ANCs with λ-CRG was successful and had improvements on the degradation of it. The temperatures of degradation observed by the thermograms and DSC graphs in the BbE, had shifts to higher temperatures, in the BbE-λ-CRG insoluble complexes, therefore, it was concluded that the complexation had a positive impact on the thermal stability of this extract. *In vitro* release was also studied, to understand how ANCs could behave under different pH and salt compositions. Results showed that release at each time mark, from BbE-λ-CRG insoluble complexes in MES and pH=5.4 was constant from the 1-hour mark until the 8-hour mark. PBS and pH=1.7 had a decrease on the release of ANCs as time passed by, which may be resultant from the high effect of dilution in the release, compared to the diffusion. At pH=7.4, the release was trending to a higher degree as time increased. Furthermore, the salt composition and ionic strength had a direct influence on the release of ANCs from the BbE-λ-CRG complexes. From the fitting of the data to the Korsmeyer-Peppas model, it was possible to determine that in pH=5.4, pH=7.4 and MES, the release was following the model of the Fick's diffusion.

Concerning the formation of the BbE-λ-CRG complexes, it would be useful to perform solid-state nuclear magnetic resonance to find more information about the type of ANCs structures in equilibrium that contributes on the complexation. In addition, it might reveal information about how the electrostatic interaction takes place. The use of fruit extracts that has a related composition to blackberry, for example, blueberries and raspberries, can be beneficial in the discovery of new sources to produce insoluble complexes. In addition, it would be important to explore novel extraction methods, for instance, using ionic liquids or deep eutectic solvents. Bioaccessibility studies of ANCs released from the BbE-λ-CRG complexes and the complexes themselves would be important to perform. The release profile of ANCs in other systems than water-based ones, and the stability of these polyphenols in simulated digestive systems will give a detailed information about the bioavailability of ANCs. A detailed physical characterization of the insoluble complexes, beginning with swelling assays, could be beneficial to a better understanding of how the release of ANCs occurs when solid insoluble complexes are in an aqueous medium. The natural tendency of aggregation by solid insoluble complexes could be helpful on the formation of biodegradable films, that can be characterized in terms of its rheology.

Application of these insoluble complexes in the food industry, can be view as the production of bio-based films for functional packaging and food preservation. On the other hand, it could be applied as an insoluble pigment in food products, a mechanism to increase ANCs bioaccessibility, or a drug delivery system.

References

Alavi, S., & Mortazavi, S. A. (2018). Freeze-Dried K-Carrageenan/Chitosan Polyelectrolyte Complex-Based Insert: A Novel Intranasal Delivery System for Sumatriptan Succinate. *Iran J Pharm Res*, *17*(4), 1172-1181.

Albert, C., Codină, G. G., Héjja, M., András, C. D., Chetrariu, A., & Dabija, A. (2022). Study of Antioxidant Activity of Garden Blackberries (Rubus fruticosus L.) Extracts Obtained with Different Extraction Solvents. *Applied Sciences*, *12*(8), 4004.

Albuquerque, B. R., Oliveira, M. B. P. P., Barros, L., & Ferreira, I. C. F. R. (2021). Could fruits be a reliable source of food colorants? Pros and cons of these natural additives. *Critical Reviews in Food Science and Nutrition*, *61*(5), 805-835.

Alexandra Pazmiño-Durán, E., Mónica Giusti, M., Wrolstad, R. E., & Glória, M. B. A. (2001). Anthocyanins from Oxalis triangularis as potential food colorants. *Food Chemistry*, *75*(2), 211-216.

Amarowicz, R., Carle, R., Dongowski, G., Durazzo, A., Galensa, R., Kammerer, D., Maiani, G., & Piskula, M. K. (2009). Influence of postharvest processing and storage on the content of phenolic acids and flavonoids in foods. *Molecular nutrition & food research*, *53*(S2), S151-S183.

Andersen, Ø. M., & Jordheim, M. (2013). Basic anthocyanin chemistry and dietary sources. *Anthocyanins in health and disease*, *1*, 13-89.

Anitha, A., Deepagan, V. G., Divya Rani, V. V., Menon, D., Nair, S. V., & Jayakumar, R. (2011). Preparation, characterization, in vitro drug release and biological studies of curcumin loaded dextran sulphate–chitosan nanoparticles. *Carbohydrate Polymers*, *84*(3), 1158-1164.

Balasundram, N., Sundram, K., & Samman, S. (2006). Phenolic compounds in plants and agri-industrial by-products: Antioxidant activity, occurrence, and potential uses. *Food Chemistry*, *99*(1), 191-203.

Bellich, B., D'Agostino, I., Semeraro, S., Gamini, A., & Cesàro, A. (2016). "The Good, the Bad and the Ugly" of Chitosans. *Mar Drugs*, *14*(5).

Bhattacharjee, S. (2016). DLS and zeta potential – What they are and what they are not? *Journal of Controlled Release*, *235*, 337-351.

Bientinesi, E., Lulli, M., Becatti, M., Ristori, S., Margheri, F., & Monti, D. (2022). Doxorubicin-induced senescence in normal fibroblasts promotes in vitro tumour cell growth and invasiveness: The role of Quercetin in modulating these processes. *Mechanisms of Ageing and Development*, *206*, 111689.

Blocher McTigue, W. C., & Perry, S. L. (2020). Protein Encapsulation Using Complex Coacervates: What Nature Has to Teach Us. *Small*, *16*(27), 1907671.

Borges, A., Freitas, V., Mateus, N., Fernandes, I., & Oliveira, J. (2020). Solid Lipid Nanoparticles as Carriers of Natural Phenolic Compounds. *Antioxidants (Basel)*, *9*(10).

Bradford, M. M. (1976). A rapid and sensitive method for the quantitation of microgram quantities of protein utilizing the principle of protein-dye binding. *Analytical Biochemistry*, *72*(1), 248-254.

Brouillard, R. (1982). Chapter 1 - Chemical Structure of Anthocyanins. In P. Markakis (Ed.), *Anthocyanins As Food Colors* (pp. 1-40). Academic Press.

Brouillard, R., & Dubois, J.-E. (1977). Mechanism of the structural transformations of anthocyanins in acidic media. *Journal of the American Chemical Society*, *99*(5), 1359-1364.

Brown, C. R. (2005). Antioxidants in potato [Review]. *American Journal of Potato Research*, *82*(2), 163-172.

Bueno, J. M., Sáez-Plaza, P., Ramos-Escudero, F., Jiménez, A. M., Fett, R., & Asuero, A. G. (2012). Analysis and Antioxidant Capacity of Anthocyanin Pigments. Part II: Chemical Structure, Color, and Intake of Anthocyanins. *Critical Reviews in Analytical Chemistry*, *42*(2), 126-151.

Buriuli, M., & Verma, D. (2017). Polyelectrolyte Complexes (PECs) for Biomedical Applications. In A. Tripathi & J. S. Melo (Eds.), *Advances in Biomaterials for Biomedical Applications* (pp. 45-93). Springer Singapore.

Carocho, M., Morales, P., & Ferreira, I. (2015). Natural food additives: Quo vadis? [Review]. *Trends in Food Science & Technology*, *45*(2), 284-295.

Castañeda-Ovando, A., Pacheco-Hernández, M. d. L., Páez-Hernández, M. E., Rodríguez, J. A., & Galán-Vidal, C. A. (2009). Chemical studies of anthocyanins: A review. *Food Chemistry*, *113*(4), 859-871.

Cavalcanti, R. N., Santos, D. T., & Meireles, M. A. A. (2011). Non-thermal stabilization mechanisms of anthocyanins in model and food systems—An overview. *Food Research International*, *44*(2), 499-509.

Chandrasekara, A., & Shahidi, F. (2010). Content of insoluble bound phenolics in millets and their contribution to antioxidant capacity. *J Agric Food Chem*, *58*(11), 6706-6714.

Chen, G., Li, Y., Wang, W., & Deng, L. (2018). Bioactivity and pharmacological properties of α-mangostin from the mangosteen fruit: a review. *EXPERT OPINION ON THERAPEUTIC PATENTS*, *28*(5), 415-427.

Ćirić, A., Medarević, Đ., Čalija, B., Dobričić, V., Mitrić, M., & Djekic, L. (2020). Study of chitosan/xanthan gum polyelectrolyte complexes formation, solid state and influence on ibuprofen release kinetics. *International Journal of Biological Macromolecules*, *148*, 942-955.

Colombo, P. (1993). Swelling-controlled release in hydrogel matrices for oral route. *Advanced Drug Delivery Reviews*, *11*(1-2), 37-57.

Cruz, L., Basílio, N., Mateus, N., Pina, F., & de Freitas, V. (2015). Characterization of Kinetic and Thermodynamic Parameters of Cyanidin-3-glucoside Methyl and Glucuronyl Metabolite Conjugates. *The Journal of Physical Chemistry B*, *119*(5), 2010-2018.

de Souza, H. K. S., Bai, G., Gonçalves, M. d. P., & Bastos, M. (2009). Whey protein isolate–chitosan interactions: A calorimetric and spectroscopy study. *Thermochimica Acta*, *495*(1), 108-114.

Dordevic, V., Balanc, B., Belscak-Cvitanovic, A., Levic, S., Trifkovic, K., Kalusevic, A., Kostic, I., Komes, D., Bugarski, B., & Nedovic, V. (2015). Trends in Encapsulation Technologies for Delivery of Food Bioactive Compounds [Review]. *Food Engineering Reviews*, *7*(4), 452-490.

Dragan, E. S., & Schwarz, S. (2004). Polyelectrolyte complexes. VI. Polycation structure, polyanion molar mass, and polyion concentration effects on complex nanoparticles based on poly(sodium 2-acrylamido-2-methylpropanesulfonate). *Journal of Polymer Science Part A: Polymer Chemistry*, *42*(10), 2495-2505.

Durazzo, A., Lucarini, M., Souto, E. B., Cicala, C., Caiazzo, E., Izzo, A. A., Novellino, E., & Santini, A. (2019). Polyphenols: A concise overview on the chemistry, occurrence, and human health. *Phytotherapy Research*, *33*(9), 2221-2243.

Echegaray, N., Munekata, P. E. S., Gullón, P., Dzuvor, C. K. O., Gullón, B., Kubi, F., & Lorenzo, J. M. (2020). Recent advances in food products fortification with anthocyanins. *Critical Reviews in Food Science and Nutrition*, 1-15.

Eiro, M. J., & Heinonen, M. (2002). Anthocyanin Color Behavior and Stability during Storage: Effect of Intermolecular Copigmentation. *Journal of Agricultural and Food Chemistry*, *50*(25), 7461-7466.

Ekalu, A., & Habila, J. D. (2020). Flavonoids: isolation, characterization, and health benefits [Review]. *Beni-Suef University Journal of Basic and Applied Sciences*, *9*(1), Article 45.

Ersus, S., & Yurdagel, U. (2007). Microencapsulation of anthocyanin pigments of black carrot (Daucus carota L.) by spray drier. *Journal of Food Engineering*, *80*(3), 805-812.

Espinosa-Andrews, H., Enríquez-Ramírez, K. E., García-Márquez, E., Ramírez-Santiago, C., Lobato-Calleros, C., & Vernon-Carter, J. (2013). Interrelationship between the

zeta potential and viscoelastic properties in coacervates complexes. *Carbohydrate Polymers*, *95*(1), 161-166.

Esposito, D., Damsud, T., Wilson, M., Grace, M. H., Strauch, R., Li, X., Lila, M. A., & Komarnytsky, S. (2015). Black Currant Anthocyanins Attenuate Weight Gain and Improve Glucose Metabolism in Diet-Induced Obese Mice with Intact, but Not Disrupted, Gut Microbiome [Article]. *Journal of Agricultural and Food Chemistry*, *63*(27), 6172-6180.

Fang, J.-L., Luo, Y., Yuan, K., Guo, Y., & Jin, S.-H. (2020). Preparation and evaluation of an encapsulated anthocyanin complex for enhancing the stability of anthocyanin. *LWT*, *117*, 108543.

Fernandes, A., Oliveira, J., Fonseca, F., Ferreira-da-Silva, F., Mateus, N., Vincken, J.-P., & de Freitas, V. (2020). Molecular binding between anthocyanins and pectic polysaccharides – Unveiling the role of pectic polysaccharides structure. *Food Hydrocolloids*, *102*, 105625.

Fernandes, A., Rocha, M. A., Santos, L. M., Brás, J., Oliveira, J., Mateus, N., & de Freitas, V. (2018). Blackberry anthocyanins: β-Cyclodextrin fortification for thermal and gastrointestinal stabilization. *Food Chemistry*, *245*, 426-431.

Ferreira, N. N., Perez, T. A., Pedreiro, L. N., Prezotti, F. G., Boni, F. I., Cardoso, V. M. d. O., Venâncio, T., & Gremião, M. P. D. (2017). A novel pH-responsive hydrogel-based on calcium alginate engineered by the previous formation of polyelectrolyte complexes (PECs) intended to vaginal administration. *Drug Development and Industrial Pharmacy*, *43*(10), 1656-1668.

Fossen, T., Andersen, O. M., Ovstedal, D. O., Pedersen, A. T., & Raknes, A. (1996). Characteristic anthocyanin pattern from onions and other Allium spp [Article]. *Journal of food science*, *61*(4), 703-706.

Fu, X., Belwal, T., He, Y., Xu, Y., Li, L., & Luo, Z. (2020). Interaction and binding mechanism of cyanidin-3-O-glucoside to ovalbumin in varying pH conditions: A spectroscopic and molecular docking study. *Food Chemistry*, *320*, 126616.

Gérard, V., Ay, E., Graff, B., Morlet-Savary, F., Galopin, C., Mutilangi, W., & Lalevée, J. (2019). Ascorbic Acid Derivatives as Potential Substitutes for Ascorbic Acid To Reduce Color Degradation of Drinks Containing Ascorbic Acid and Anthocyanins from Natural Extracts. *Journal of Agricultural and Food Chemistry*, *67*(43), 12061-12071.

Gharanjig, H., Gharanjig, K., Farzi, G., Hosseinnezhad, M., & Jafari, S. M. (2020). Novel complex coacervates based on Zedo gum, cress seed gum and gelatin for loading of natural anthocyanins [Article]. *International Journal of Biological Macromolecules*, *164*, 3349-3360.

Hamed, I., Özogul, F., & Regenstein, J. M. (2016). Industrial applications of crustacean by-products (chitin, chitosan, and chitooligosaccharides): A review. *Trends in Food Science and Technology*, *48*, 40-50.

He, J., & Giusti, M. M. (2010). Anthocyanins: Natural Colorants with Health-Promoting Properties. *Annual Review of Food Science and Technology*, *1*(1), 163-187.

Hollman, P. C. H., & Katan, M. B. (1999). Dietary Flavonoids: Intake, Health Effects and Bioavailability. *Food and Chemical Toxicology*, *37*(9), 937-942.

Huang, G.-Q., Sun, Y.-T., Xiao, J.-X., & Yang, J. (2012). Complex coacervation of soybean protein isolate and chitosan. *Food Chemistry*, *135*(2), 534-539.

Huang, Y., Zhou, S., Zhao, G., & Ye, F. (2021). Destabilisation and stabilisation of anthocyanins in purple-fleshed sweet potatoes: A review. *Trends in Food Science & Technology*, *116*, 1141-1154.

Jeong, D., & Na, K. (2012). Chondroitin sulfate based nanocomplex for enhancing the stability and activity of anthocyanin. *Carbohydr Polym*, *90*(1), 507-515.

Ji, Y., An, Q., Zhao, Q., Chen, H., Qian, J., & Gao, C. (2010). Fabrication and performance of a new type of charged nanofiltration membrane based on polyelectrolyte complex. *Journal of Membrane Science*, *357*(1-2), 80-89.

Jordheim, M. (2007). Isolation, identification and properties of pyranoanthocyanins and anthocyanin forms.

Jumaah, F., Mobarak, N., Ahmad, A., Ghani, M., & Rahman, M. (2015). Derivative of iota-carrageenan as solid polymer electrolyte. *Ionics*, *21*(5), 1311-1320.

Karimi, M. H., Mahdavinia, G. R., & Massoumi, B. (2018). pH-controlled sunitinib anticancer release from magnetic chitosan nanoparticles crosslinked with κ-carrageenan. *Materials Science and Engineering: C*, *91*, 705-714.

Kausar, H., Jeyabalan, J., Aqil, F., Chabba, D., Sidana, J., Singh, I. P., & Gupta, R. C. (2012). Berry anthocyanidins synergistically suppress growth and invasive potential of human non-small-cell lung cancer cells. *Cancer Letters*, *325*(1), 54-62.

Khan, N. A., Khan, A., Ullah, R., Ullah, M., Alotaibi, A., Ullah, R., & Haider, A. (2022). Preparation and Characterization of Hydrophilic Polymer Based Sustained-Release Matrix Tablets of a High Dose Hydrophobic Drug. *Polymers*, *14*(10), 1985.

Khoo, H. E., Azlan, A., Tang, S. T., & Lim, S. M. (2017). Anthocyanidins and anthocyanins: colored pigments as food, pharmaceutical ingredients, and the potential health benefits [Review]. *Food & Nutrition Research*, *61*, 1-21, Article 1361779.

Klimaviciute, R., Navikaite, V., Jakstas, V., & Ivanauskas, L. (2015). Complexes of dextran sulfate and anthocyanins from Vaccinium myrtillus: Formation and stability. *Carbohydr Polym*, *129*, 70-78.

Kong, J.-M., Chia, L.-S., Goh, N.-K., Chia, T.-F., & Brouillard, R. (2003). Analysis and biological activities of anthocyanins. *Phytochemistry*, *64*(5), 923-933.

Korkina, L., & Kostyuk, V. (2012). Biotechnologically Produced Secondary Plant Metabolites for Cancer Treatment and Prevention [Review]. *Current Pharmaceutical Biotechnology*, *13*(1), 265-275.

Korsmeyer, R. W., Gurny, R., Doelker, E., Buri, P., & Peppas, N. A. (1983). Mechanisms of solute release from porous hydrophilic polymers. *International journal of pharmaceutics*, *15*(1), 25-35.

Krga, I., & Milenkovic, D. (2019). Anthocyanins: From Sources and Bioavailability to Cardiovascular-Health Benefits and Molecular Mechanisms of Action [Review]. *Journal of Agricultural and Food Chemistry*, *67*(7), 1771-1783.

Krizova, L., Dadakova, K., Kasparovska, J., & Kasparovsky, T. (2019). Isoflavones [Review]. *Molecules*, *24*(6), Article 1076.

Lee, J. S., Kim, Y. R., Song, I. G., Ha, S.-J., Kim, Y. E., Baek, N.-I., & Hong, E. K. (2015). Cyanidin-3-glucoside isolated from mulberry fruit protects pancreatic β-cells against oxidative stress-induced apoptosis. *Int J Mol Med*, *35*(2), 405-412.

Li, H., Zhu, X., Xu, J., Peng, W., Zhong, S., & Wang, Y. (2016). The combination of adsorption by functionalized halloysite nanotubes and encapsulation by polyelectrolyte coatings for sustained drug delivery. *Rsc Advances*, *6*(59), 54463-54470.

Li, L., Ni, R., Shao, Y., & Mao, S. R. (2014). Carrageenan and its applications in drug delivery [Review]. *Carbohydrate Polymers*, *103*, 1-11.

Liou, C.-J., Lee, Y.-K., Ting, N.-C., Chen, Y.-L., Shen, S.-C., Wu, S.-J., & Huang, W.-C. (2019). Protective Effects of Licochalcone A Ameliorates Obesity and Non-Alcoholic Fatty Liver Disease Via Promotion of the Sirt-1/AMPK Pathway in Mice Fed a High-Fat Diet. *Cells*, *8*(5).

Liu, W. Y., Liou, S. S., Hong, T. Y., & Liu, I. M. (2017). Protective Effects of Hesperidin (Citrus Flavonone) on High Glucose Induced Oxidative Stress and Apoptosis in a Cellular Model for Diabetic Retinopathy. *Nutrients*, *9*(12), Article 1312.

Mahdavi, S. A., Jafari, S. M., Assadpoor, E., & Dehnad, D. (2016). Microencapsulation optimization of natural anthocyanins with maltodextrin, gum Arabic and gelatin [Article]. *International Journal of Biological Macromolecules*, *85*, 379-385.

Marques, C., Fernandes, I., Norberto, S., Sá, C., Teixeira, D., de Freitas, V., Mateus, N., Calhau, C., & Faria, A. (2016). Pharmacokinetics of blackberry anthocyanins consumed with or without ethanol: A randomized and crossover trial. *Molecular nutrition & food research*, *60*(11), 2319-2330.

Martín-Del-Campo, A., Fermín-Jiménez, J. A., Fernández-Escamilla, V. V., Escalante-García, Z. Y., Macías-Rodríguez, M. E., & Estrada-Girón, Y. (2021). Improved extraction of carrageenan from red seaweed (Chondracantus canaliculatus) using ultrasound-assisted methods and evaluation of the yield, physicochemical properties and functional groups. *Food Sci Biotechnol*, *30*(7), 901-910.

Mastroiacovo, D., Kwik-Uribe, C., Grassi, D., Necozione, S., Raffaele, A., Pistacchio, L., Righetti, R., Bocale, R., Lechiara, M. C., Marini, C., Ferri, C., & Desideri, G. (2015). Cocoa flavanol consumption improves cognitive function, blood pressure control, and metabolic profile in elderly subjects: the Cocoa, Cognition, and Aging (CoCoA) Study-a randomized controlled trial. *AMERICAN JOURNAL OF CLINICAL NUTRITION*, *101*(3), 538-548.

McHugh, D. J. (2003). A guide to the seaweed industry.

Meka, V. S., Sing, M. K. G., Pichika, M. R., Nali, S. R., Kolapalli, V. R. M., & Kesharwani, P. (2017). A comprehensive review on polyelectrolyte complexes. *Drug Discovery Today*, *22*(11), 1697-1706.

Meng, G., Chai, K., Li, X., Zhu, Y., & Huang, W. (2016). Luteolin exerts pro-apoptotic effect and anti-migration effects on A549 lung adenocarcinoma cells through the activation of MEK/ERK signaling pathway. *Chemico-Biological Interactions*, *257*, 26-34.

Mohamed, S. A. A., El-Sakhawy, M., & El-Sakhawy, M. A. M. (2020). Polysaccharides, Protein and Lipid -Based Natural Edible Films in Food Packaging: A Review. *Carbohydrate Polymers*, *238*, Article 116178.

Montibeller, M. J., de Lima Monteiro, P., Tupuna-Yerovi, D. S., Rios, A. d. O., & Manfroi, V. (2018). Stability assessment of anthocyanins obtained from skin grape applied in kefir and carbonated water as a natural colorant. *Journal of Food Processing and Preservation*, *42*(8), e13698.

Navikaite, V., Simanaviciute, D., Klimaviciute, R., Jakstas, V., & Ivanauskas, L. (2016). Interaction between κ-and ι-carrageenan and anthocyanins from Vaccinium myrtillus. *Carbohydrate Polymers*, *148*, 36-44.

Necas, J., & Bartosikova, L. (2013). Carrageenan: a review [Review]. *Veterinarni Medicina*, *58*(4), 187-205.

Oancea, S. (2021). A review of the current knowledge of thermal stability of anthocyanins and approaches to their stabilization to heat. *Antioxidants*, *10*(9), 1337.

Oz, H. S. (2017). Chronic Inflammatory Diseases and Green Tea Polyphenols [Review]. *Nutrients*, *9*(6), Article 561.

Pacheco-Quito, E. M., Ruiz-Caro, R., & Veiga, M. D. (2020). Carrageenan: Drug Delivery Systems and Other Biomedical Applications [Review]. *Marine Drugs*, *18*(11), Article 583.

Panche, A. N., Diwan, A. D., & Chandra, S. R. (2016). Flavonoids: an overview. *Journal of nutritional science*, *5*, e47-e47.

Pandey, K. B., & Rizvi, S. I. (2009). Plant polyphenols as dietary antioxidants in human health and disease. *Oxidative Medicine and Cellular Longevity*, *2*(5), 270-278.

Pina, F. (2014). Chemical Applications of Anthocyanins and Related Compounds. A Source of Bioinspiration. *Journal of Agricultural and Food Chemistry*, *62*(29), 6885-6897.

Polat, T. G., Duman, O., & Tunç, S. (2020). Preparation and characterization of environmentally friendly agar/κ-carrageenan/montmorillonite nanocomposite hydrogels. *Colloids and Surfaces A: Physicochemical and Engineering Aspects*, *602*, 124987.

Prior, R. L., & Wu, X. L. (2006). Anthocyanins: Structural characteristics that result in unique metabolic patterns and biological activities [Review]. *Free Radical Research*, *40*(10), 1014-1028.

Quan, W., He, W., Lu, M., Yuan, B., Zeng, M., Gao, D., Qin, F., Chen, J., & He, Z. (2019). Anthocyanin composition and storage degradation kinetics of anthocyanins-based natural food colourant from purple-fleshed sweet potato. *International Journal of Food Science & Technology*, *54*(8), 2529-2539.

Ravanfar, R., Tamaddon, A. M., Niakousari, M., & Moein, M. R. (2016). Preservation of anthocyanins in solid lipid nanoparticles: Optimization of a microemulsion dilution method using the Placket–Burman and Box–Behnken designs. *Food Chemistry*, *199*, 573-580.

Renaud, S. d., & de Lorgeril, M. (1992). Wine, alcohol, platelets, and the French paradox for coronary heart disease. *The Lancet*, *339*(8808), 1523-1526.

Rodriguez-Garcia, C., Sanchez-Quesada, C., Toledo, E., Delgado-Rodriguez, M., & Gaforio, J. J. (2019). Naturally Lignan-Rich Foods: A Dietary Tool for Health Promotion? [Review]. *Molecules*, *24*(5), Article 917.

Rodriguez-Saona, L., Giusti, M., & Wrolstad, R. (1999). Color and pigment stability of red radish and red-fleshed potato anthocyanins in juice model systems. *Journal of food science*, *64*(3), 451-456.

Rumyantsev, A. M., Jackson, N. E., & De Pablo, J. J. (2021). Polyelectrolyte Complex Coacervates: Recent Developments and New Frontiers. *Annual Review of Condensed Matter Physics*, *12*, 155-176.

Sagar, N. A., Pareek, S., Sharma, S., Yahia, E. M., & Lobo, M. G. (2018). Fruit and vegetable waste: Bioactive compounds, their extraction, and possible utilization. *Comprehensive Reviews in Food Science and Food Safety*, *17*(3), 512-531.

Sarkar, R., Dutta, A., Patra, A., & Saha, S. (2021). Bio-inspired biopolymeric coacervation for entrapment and targeted release of anthocyanin [Article]. *Cellulose*, *28*(1), 377-388.

Shaddel, R., Hesari, J., Azadmard-Damirchi, S., Hamishehkar, H., Fathi-Achachlouei, B., & Huang, Q. (2018). Use of gelatin and gum Arabic for encapsulation of black raspberry anthocyanins by complex coacervation [Article]. *International Journal of Biological Macromolecules*, *107*, 1800-1810.

Shahidi, F. (2012). *Dried fruits: phytochemicals and health effects*. John Wiley & Sons.

Shchipunov, Y. A., & Postnova, I. V. (2009). Water-Soluble Polyelectrolyte Complexes of Oppositely Charged Polysaccharides. *Composite Interfaces*, *16*(4-6), 251-279.

Shih, F.-Y., Su, I.-J., Chu, L.-L., Lin, X., Kuo, S.-C., Hou, Y.-C., & Chiang, Y.-T. (2018). Development of Pectin-Type B Gelatin Polyelectrolyte Complex for Curcumin Delivery in Anticancer Therapy. *International Journal of Molecular Sciences*, *19*(11).

Shovsky, A., Varga, I., Makuška, R., & Claesson, P. M. (2009). Formation and Stability of Water-Soluble, Molecular Polyelectrolyte Complexes: Effects of Charge Density, Mixing Ratio, and Polyelectrolyte Concentration. *Langmuir*, *25*(11), 6113-6121.

Siepmann, J., & Siepmann, F. (2012). Modeling of diffusion controlled drug delivery. *Journal of Controlled Release*, *161*(2), 351-362.

Singhvi, G., & Singh, M. (2011). In-vitro drug release characterization models. *Int J Pharm Stud Res*, *2*(1), 77-84.

Singleton, V. L., & Rossi, J. A. (1965). Colorimetry of total phenolics with phosphomolybdic-phosphotungstic acid reagents. *American journal of Enology and Viticulture*, *16*(3), 144-158.

Soares, S., Sousa, A., Mateus, N., & de Freitas, V. (2012). Effect of condensed tannins addition on the astringency of red wines. *Chemical senses*, *37*(2), 191-198.

Song, Y., Liu, L., Shen, H., You, J., & Luo, Y. (2011). Effect of sodium alginate-based edible coating containing different anti-oxidants on quality and shelf life of refrigerated bream (Megalobrama amblycephala). *Food control*, *22*(3-4), 608-615.

Souza, H. K. S., Mateus, N., de Freitas, V., Gonçalves, M. P., & Cruz, L. (2020). Chemical/Color Stability and Rheological Properties of Cyanidin-3-Glucoside in Deep Eutectic Solvents as a Gateway to Design Task-Specific Bioactive Compounds. *ACS Sustainable Chemistry & Engineering*, *8*(43), 16184-16196.

Sun, Z., Huang, Z., & Zhang, D. D. (2009). Phosphorylation of Nrf2 at multiple sites by MAP kinases has a limited contribution in modulating the Nrf2-dependent antioxidant response. *Plos One*, *4*(8), e6588.

Supramaniam, J., Adnan, R., Mohd Kaus, N. H., & Bushra, R. (2018). Magnetic nanocellulose alginate hydrogel beads as potential drug delivery system. *Int J Biol Macromol*, *118*(Pt A), 640-648.

Susanti, I., Wijaya, H., Hasanah, F., & Heryani, S. (2018). Copigmentation Of Anthocyanin Extract of Purple Sweet Potatoes (Ipomea Batatas L.) Using Ferulic Acid And Tannic Acid. *IOP Conference Series: Earth and Environmental Science*, *116*, 012006.

Tajik, N., Tajik, M., Mack, I., & Enck, P. (2017). The potential effects of chlorogenic acid, the main phenolic components in coffee, on health: a comprehensive review of the literature. *European Journal of Nutrition*, *56*(7), 2215-2244.

Tapia, C., Escobar, Z., Costa, E., Sapag-Hagar, J., Valenzuela, F., Basualto, C., Nella Gai, M. a., & Yazdani-Pedram, M. (2004). Comparative studies on polyelectrolyte complexes and mixtures of chitosan–alginate and chitosan–carrageenan as prolonged diltiazem clorhydrate release systems. *European Journal of Pharmaceutics and Biopharmaceutics*, *57*(1), 65-75.

Tavares, L., Souza, H. K. S., Gonçalves, M. P., & Rocha, C. M. R. (2021). Physicochemical and microstructural properties of composite edible film obtained by complex coacervation between chitosan and whey protein isolate. *Food Hydrocolloids*, *113*, 106471.

Teixeira-Costa, B. E., Pereira, B. C. S., Lopes, G. K., & Andrade, C. T. (2020). Encapsulation and antioxidant activity of assai pulp oil (Euterpe oleracea) in chitosan/alginate polyelectrolyte complexes. *Food Hydrocolloids*, *109*, 106097.

Thangavel, P., Puga-Olguín, A., Rodríguez-Landa, J. F., & Zepeda, R. C. (2019). Genistein as Potential Therapeutic Candidate for Menopausal Symptoms and Other Related Diseases. *Molecules*, *24*(21).

Thünemann, A. F., Müller, M., Dautzenberg, H., Joanny, J.-F., & Löwen, H. (2004). Polyelectrolyte Complexes. In M. Schmidt (Ed.), *Polyelectrolytes with Defined Molecular Architecture II* (pp. 113-171). Springer Berlin Heidelberg.

Timilsena, Y. P., Akanbi, T. O., Khalid, N., Adhikari, B., & Barrow, C. J. (2019). Complex coacervation: Principles, mechanisms and applications in microencapsulation [Review]. *International Journal of Biological Macromolecules*, *121*, 1276-1286.

Trouillas, P., Sancho-García, J. C., De Freitas, V., Gierschner, J., Otyepka, M., & Dangles, O. (2016). Stabilizing and Modulating Color by Copigmentation: Insights from Theory and Experiment. *Chemical Reviews*, *116*(9), 4937-4982.

Tsai, H.-Y., Ho, C.-T., & Chen, Y.-K. (2017). Biological actions and molecular effects of resveratrol, pterostilbene, and 3′-hydroxypterostilbene. *Journal of Food and Drug Analysis*, *25*(1), 134-147.

Vasconcelos, N. G., Croda, J., & Simionatto, S. (2018). Antibacterial mechanisms of cinnamon and its constituents: A review. *Microbial Pathogenesis*, *120*, 198-203.

Wallace, T. C., & Giusti, M. M. (2008). Determination of color, pigment, and phenolic stability in yogurt systems colored with nonacylated anthocyanins from Berberis boliviana L. as compared to other natural/synthetic colorants. *Journal of food science*, *73*(4), C241-C248.

Winkel-Shirley, B. (2001). Flavonoid biosynthesis. A colorful model for genetics, biochemistry, cell biology, and biotechnology. *Plant physiology*, *126*(2), 485-493.

Wrolstad, R. E., Durst, R. W., & Lee, J. (2005). Tracking color and pigment changes in anthocyanin products. *Trends in Food Science & Technology*, *16*(9), 423-428.

Yan, F., Chen, Y., Azat, R., & Zheng, X. (2017). Mulberry Anthocyanin Extract Ameliorates Oxidative Damage in HepG2 Cells and Prolongs the Lifespan of Caenorhabditis elegans through MAPK and Nrf2 Pathways. *Oxidative Medicine and Cellular Longevity*, *2017*, 7956158.

Zaitsev, S., Cartier, R., Vyborov, O., Sukhorukov, G., Paulke, B.-R., Haberland, A., Parfyonova, Y., Tkachuk, V., & Böttger, M. (2004). Polyelectrolyte nanoparticles mediate vascular gene delivery. *Pharmaceutical Research*, *21*(9), 1656-1661.

Zhai, Y., & Zhai, G. (2014). Advances in lipid-based colloid systems as drug carrier for topic delivery. *Journal of Controlled Release*, *193*, 90-99.

Attachments

Table A1- Percentage of release expressed as mean ± SD; For each row, samples with the same symbol (*) do not present statistical differences (p>0.05).

Time (h)	**Release rate (%)**				
	H_2O pH = 1.7	**MES (10 mM)**	**PBS (10 mM)**	**H_2O pH = 5.4**	**H_2O pH = 7.4**
0	0.0 ± 0.0	0.0 ± 0.0	0.0 ± 0.0	0.0 ± 0.0	0.0 ± 0.0
0.5	5.5* ± 0.1	2.7** ± 0.0	7.9 ± 0.1	3.8*,** ± 0.2	5.3* ± 0.1
1	5.6*,** ± 0.1	3.8* ± 0.1	9.8 ± 0.1	4.7*,** ± 0.2	6.7** ± 0.2
2	4.5*± 0.1	3.9* ± 0.2	14.6 ± 0.1	5.0* ± 0.2	7.7* ± 0.3
3	3.4* ± 0.1	4.2* ± 0.3	13.9** ± 0.1	4.8* ± 0.1	8.2*,** ± 0.2
4	2.6* ± 0.1	4.6* ± 0.3	12.4** ± 0.1	5.1* ± 0.1	8.7*,** ± 0.2
5	1.7* ± 0.1	4.8* ± 0.4	10.6** ± 0.1	5.1* ± 0.0	9.4** ± 0.3
6	1.1* ± 0.2	5.1*,** ± 0.5	9.2** ± 0.1	4.9*,** ± 0.0	10.1** ± 0.3
7	0.5* ± 0.3	5.3*,** ± 0.5	7.1** ± 0.1	4.8*,** ± 0.0	10.8** ± 0.3
8	0.0* ± 0.3	5.2* ± 0.5	5.3*,** ± 0.1	4.4* ± 0.1	11.1** ± 0.3

Table A2- FTIR-ATR bands recorded in BbE, λ-CRG and BbE-λ-CRG complexes. ν refers to streching vibrations; δ refers to bending vibrations.

Type of band	Wavenumber (cm^{-1})		
	BbE	**λ-CRG**	**BbE-λ-CRG**
ν (O-H)	3234	3400	3251
ν (C-H)	2915	n.p	2882
ν (C-H) aldehyde	2815	n.p	2848
ν (C=O) benzopyran	1685	n.p	1692
ν (C=C)	1632	1617	1634
δ (CH_2) sp^2	1507	n.p	1510
δ (CH_3) sp^3	1438	n.p	1436
δ (O-H) phenol	1310	n.p	1321
ν (C-O-H)	1169	1207	1175
ν_s (O=S=O)	n.p	1220	1183
ν (C-O)	1155	n.p	n.p
ν (C-O-S) of galactose-4-sulfate	n.p	922	n.p
ν (C-O-S) of 3,6-anhydrogalactose-2-sulfate	n.p	834	n.p